TABLE OF CONTENTS

ABSTRACT

An advanced control approach (model predictive control) is applied on a wind turbine system and discussed in this project. A model of a wind turbine system is defined with respect to the dynamics it. The non-linear model is derived and validated under different type of external disturbances. Then, it is linearized for operational values that are lying on the rated region of a wind turbine. The theory of model predictive control under the receding horizon concept is examined and based on this theory; a control strategy and an optimization problem are defined. Based on them and the created model, three different MPCs are designed using an external code generation program (CVXGEN). The designed controllers are tuned under different horizon lengths and then implemented and validate that they are able to handle the system's deviations. A comparison between the designed MPCs and classic control approaches (PI) is conducted in combination with a Power Spectrum Density analysis. Then, the best fitted controller is implemented to the designed nonlinear model and compared with the proposed baseline controller. The results of the comparison are summarized to show the advantages and disadvantages of controlling simple models with advanced control methods.

ABBREVIATIONS

WT	Wind Turbine
WTG	Wind Turbine Generator
OECD	Organization for Economic Cooperation and Development
IEA	International Energy Agency
RES	Renewable Energy Systems
EU	European Union
LIDAR	LIght Detection and Ranging
MPC	Model Predictive Controller
LMPC	Linear Model Predictive Controller
NMPC	Non-linear Model Predictive Controller
PI	Proportional integral controller
ICT	Information and Communication Technology
QP	Quadratic Problem
BEM	Blade Element Theory
PSD	Power Spectra Density
DT	Discrete Time

NOMENCLATURE

$\boldsymbol{\beta}$	pitch angle [degrees]
$\boldsymbol{\omega_r}$	rotor speed [rads/s]
$\boldsymbol{\omega_g}$	generator speed [rads/s]
$\mathbf{T_g}$	generator torque [Nm]
$\mathbf{P_g}$	produced power [W]
$\mathbf{V_r}$	rotor's wind velocity [m/s]
$\mathbf{T_r}$	rotor's torque [Nm]
$\boldsymbol{\beta_{ref}}$	refer. Pitch angle [degrees]
$\mathbf{T_{g,\,ref}}$	refer. generator torque [Nm]
$\mathbf{F_T}$	thrust force [N]
$\dot{Y}_T$	fore-aft velocity
$\dot{\mathbf{m}}_V$	mass flow rate [kg/s]
$\boldsymbol{\rho}$	air density [kg/m^3]
A	cross section area [m^2]
$\mathbf{F_V}$	force in the wind []
$\mathbf{P_V}$	kinetic energy [kgm^2/s^2]
$\mathbf{C_p}$	power coefficient [unit less]
$\boldsymbol{\lambda}$	tip-speed ratio [unit less]
R	rotor's radius [m]
$\mathbf{P_r}$	rotor's produced mech. power
$\mathbf{T_r}$	rotor's generated torque [Nm]
$\mathbf{J_r}$	rotor's inertia (low shaft) [kgm^2]
$\mathbf{J_g}$	generator's inertia (high shaft) [kgm^2]
$\mathbf{K_r}$	drive train's stiffness [N/m]
$\mathbf{B_r}$	drive train's damping [Pa]
$\boldsymbol{\theta_t}$	drive train torsion [Pa]
$\boldsymbol{\tau_g}$	generator's time constant [sec]
$\mathbf{m_T}$	tower's mass [kg]
$\mathbf{K_T}$	tower's stiffness [N/m]
$\mathbf{B_T}$	tower's damping [Pa]
$\boldsymbol{\tau_p}$	pitch act. Time constant [sec]
$\mathbf{J_T}$	total inertia of drive train system [kgm^2]
$\mathbf{H_p}$	prediction horizon [sec]
$\mathbf{H_u}$	control horizon [sec]
Q, R, P	weight parameters [unit less]
S	slew rate limit [rad/s]
$\mathbf{T_s}$	sampling time [sec]

THIS PAGE LEFT BLANK ON PURPOSE

1. INTRODUCTION

The following chapter illustrates the motivation for conducting a thesis about wind turbines and their control designing using model predictive control. A small description of the background knowledge and the related work is described as well. The chapter continues with the problem statement, limitations and the structure of the thesis. In the end, the objectives and the outline of the thesis are presented.

1.1.Motivation

Energy is one of the most essential parts of our daily life. Especially, from 19th century and the industrial revolution the energy demands rising constantly and explode the last two decades. Nowadays our daily activities, such as watching television, heating our homes, surfing on the internet or even drive our cars, they all require energy consumption. Most of this is coming from fossil fuels with the known results.

Denmark, despite that is the leader among OECD countries in terms of renewable energy production, fossil fuels consumption accounts around 70% of energy consumption based on IEA reviews [1]. In the EU, countries agreed to try to reduce the fossil fuel consumption by investing in RES and limit the harmful emissions by 20% until 2020 and 80-95% by 2050 [2]. To meet these goals, investments up to hundreds of billion euros need to be done. Denmark's long term plan about energy (production and consumption) is to become independent from fossil fuels by 2050 as it was stated back in 2011 in the Energy Strategy guide published by government. These guidelines present a series of actions that will make Denmark a low-carbon energy society with stable and affordable energy supply [1]. For Denmark and for all EU countries as well, a growth in RES usage is needed instantly in order to avoid penalization for their governments and freedom from fossil fuels and their producers.

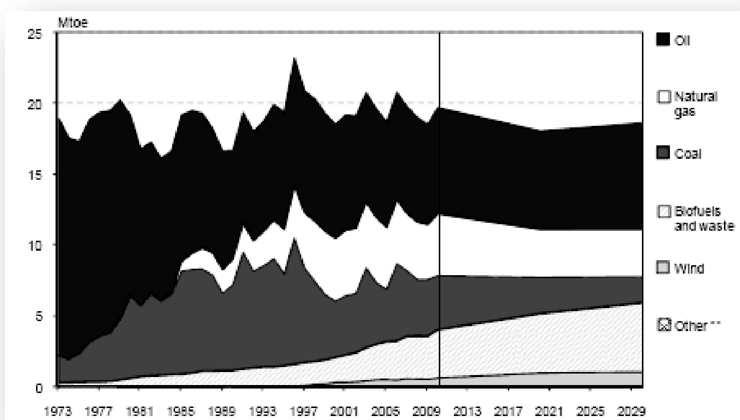

Figure 1.1 – Total primary energy supply for the EU countries, from 1973 to 2030 in total million tons of energy as equivalent [1].

As the energy demands increase, the uses of alternate sources like wind, sun, water and/or every else our planet has in abundance is becoming. RES is one solution to extract power from these sources.

Nuclear plants is also including in this solution [2]. The problem that comes with nuclear energy plants is regarding their safety. Especially after incidents like Chernobyl (April, 1986) and Fukusima (March, 2011) hosting countries feels that the idea of energy production from nuclear resources needs to be stall until a safety measurements will upgrade. For instance, Germany that used to have plenty of these plants inside their territory, shut down eight of their seventeen nuclear plants [3]. The goal is to shut down all of them by 2022 based on government's phase-out plan that was voted in 2010 and focus more in wind industry [3].

The plan of EU says that wind energy will produce one-fifth of EU's electricity production by 2020 and one-third by 2030. The final goal is the wind energy will cover up to 50% of total electricity demands for the countries of EU [4]. In order to achieve these goals, wind energy industry needs to become more cost efficient and for this reason it tries to make the WT's cost competitive. One optimization area is the placement of a WT. The size and the number of the turbines make the decision of place them difficult, as they have to change the site based on the size and number of them. This changing may lead to less favorable wind areas and hard construction conditions. Another part that can be optimized is the WT's (or wind farms) layouts and the usage of more advanced control strategies than the current existing. The problem is this case is versatile. In order to make wind energy more cost competitive the construction of bigger WTs is needed. Bigger turbines are leading to have a greater structural and mechanical load that is the challenge (mechanical) that needs to be optimized. Control plan can play a key part in this optimization. Advance control methods on one hand they can decrease the cost of energy by keeping the WT operation close to its maximum efficiency and on the other hand, at the same time, they can reduce harmful for the WT situation, such as unwanted vibrations etc. This can lead in an increase of the lifetime and therefore the energy production more cost effective [5].

Advanced control methods, controllers and sensors can be the solution to the wind energy industry problems. As the WTs getting higher, they are more affected from the wind turbulent phenomena or from other turbines that are standing in front of them (in wind farms) and are influenced by possible wake incidents. In both situations unwanted conditions that can occur to the WT can be avoid with the use of appropriate designed controllers that will be guided from the designer's needs.

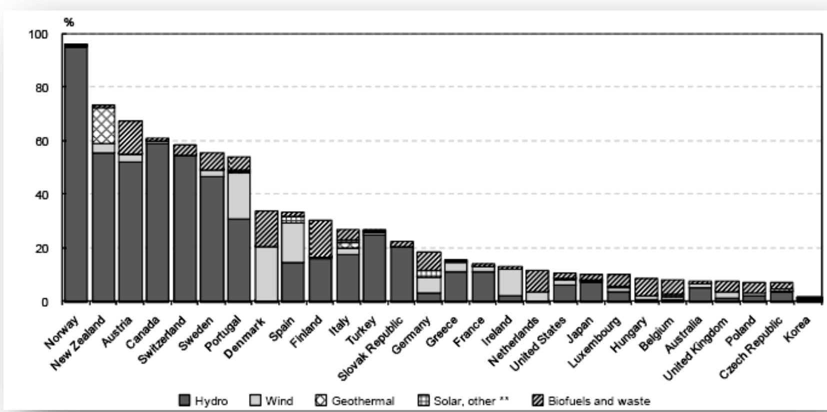

Figure 1.2 – Energy generation from RES as percentage of all generation in IEA members. Denmark produces more than 50% from wind energy [1].

1.2.Similar Work

The technology in the wind turbine industry is developing faster than ever as we saw in Ch1.1. From the fixed speed WTs in the beginning until the new age turbines with variable speed and variable pitch angle, several years of researches helped to improve them, in all of their perspectives. New mechanical designs improved the WTs' structure, evolved the size of them and at the same time improved the amount of the produced energy. In order to improve even more and make the produced power even cheaper – and finally make the wind energy the most cost effective RES solution – a maximizing in the produced energy and their operational lifetime.

Many methods of WT control exist. Extending from classical control methods, that are the most common and widely used in the industry and in real applications [5, 6, 7], to advanced control designing which have been attracting more focus lately [6, 7]. MIMO methods [8], adaptive control [9] and robust MPC [10] are some of them presented the past years. It is proven that an appropriate control of the blade pitch angle can reduce significantly the mechanical loads in the WT's structure. As the rotor size increase together with the height/size of the turbine, the effects of the wind shear also increase and the controlling through an individual pitch controller is used successfully so far [11].

Mechanical changes is an obvious but expensive solution to extend the WT lifetime but an approach that changes the control system in a WT is another option less expensive but with a lot of potential. Advanced model based control designing seems to be the present and future of WT control systems. They have the ability to include extra inputs to the control system (i.e. measurements from accelerometers or other sensors that could be placed in a wind turbine) [11]. These new measurements are used to calculate an additional pitch contribution to the already measured pitch which can help to the tower's motion damp calculation and keep the energy production in wanted levels.

New generation sensors and advance control methods, such as model predictive control, that use predictions or even knowledge of the future disturbances, are highly emerged in the wind industry. Several researches showed that using MPC control design with the use of knowledge of the future disturbance can become an asset for the WT control [12, 13 14 &15]. In the real industry, classical control methods prove their ability to maintain the operation of simple and complex systems as well, without creating big problems. Especially in wind industry PI controllers are widely used. Advanced control methods tend to overcome the classical control approach, but yet have to prove from the simpler to the most complex case that their behavior and their results have at least the same efficiency. This can be achieved by examine the results of an advanced control approach in simple and/or more complex situations.

1.3.Problem Formulation

Based on the previous sub-chapters, regarding the development of the control systems in the wind energy industry as well, we formulate our following problem:

Is model predictive control a good approach for controlling a simple wind turbine model? Is an MPC without the knowledge of the future disturbance, more robust than a simple controller? Can an advance control approach be a more appropriate control plan than a classic control approach (PI and/or PID) and eventually can make the control design procedure and the operation of a WT easier and more reliable?

The above main hypothesis is divided in several parts that are concerning the WT's model and its validation, the controller designing, the tuning of it and finally the results that will show if the hypothesis is valid. All of them are defined in the next chapters and their validation will lead to the next step and finally to the ultimate goal that is the reduction of the loads in the WT.

1.4.Limitations

Some limitations occurred during the completion of this project.

The wind turbine model used in this thesis is a reduced version based on the proposed system's dynamic behavior [16]. This version consists of WT aerodynamic and drive train part. For the design of this system, the reference power of the system was stable (see Ch. 3.9). The linearization of the created model happened around one specific point. This point is lying on the region where the turbine operates in the rated region (see Ch. 2.3).

Unfortunately, LIDAR measurements weren't provided. These kinds of measurements could have change the design procedure of the system and the controller as well. Therefore and because of their absence, the control focus will be in design an MPC controller that has no knowledge for the upcoming disturbance and it will assume it as unknown.

1.5.Objectives

The objectives of this thesis are the following:

<u>Define and validate a non-linear model</u>, similar to the well-known, used ones. This, reduced, model will be the basis for the linear model that will be part of the control design. Its validation will be done with respect to other, validated models and their dynamic behavior.

<u>Define and validate the linear model</u> that will be used for the controllers design. The model will be validated against the non-linear model's dynamic behavior. Validation will be done by disturbing the linear model away from its linearizing point.

Define the control plan, cost function and constraints based on our system needs and the controller's potential. Then, define in the external, optimization program (CVXGEN) the system's state, variables and parameters needed for the creation of the controller

Tune the parameters of the created controller in order to obtain the best/optimal output of the system states.

A comparison between the results of the designed controller and other classic controllers (PI) will be conducted with respect to control plan of both controllers. Control signal analysis will be done as well to identify the signal effect to the system

A comparison between the MPC designed controller for the defined system and the baseline controller for the proposed system will be carried as well to prove that the designed controller works as it is expected.

1.6.Thesis outline

In this section we give a brief introduction to thesis formulation and chapter description as it follow in the later stages.

Chapter 2: System description

This chapter introduces information about the WT that is used as model and the parts that the WT is divided in it. General control concept of WTGs are presenting as well. The purpose of it is to make the reader familiar with terms, conditions and concepts that later are used in the modeling procedure.

Chapter 3: Modeling of the system

This chapter includes the models of the previous referred systems. The nonlinear model is defined, derived and validated with respect to the nonlinear model presented in [16]. Additionally, the system is linearized around a point in the rated region and validated under different type of disturbances.

Chapter 4: Control plan and controller design

The development and test of the controller is presented in this chapter. The control plan together with the optimization problem of the controller is defined. The design and tuning of the model predictive controllers occur as well. A comparison of the designed controllers with respect to the system's output is happening and later the designed controller applied to the designed nonlinear model.

Chapter 5: Conclusion & future improvements

This final chapter provides a brief explanation to the way that project followed. Illustrates the results of every objective and discuss the results of the simulations. Also, future improvements based on author's experience with advance control systems will be presented as well.

2. SYSTEM DESCRIPTION

The chapter 2 introduces the different components and provides an overview of a WTG and its general control plan. This chapter aims to make the reader familiar with the critical parts of a WT and general the units that will participate in our system construction. Finally, a small description of the software that is used in order to solve as fast as possible the MPC's optimization problems is occurring as well.

2.1.Wind turbine summary

This part illustrates a HAWT and its components which are useful to the thesis completion. Generally, a WTG is a mechanical machine that takes advantage of the wind field and converts it – through the rotation of its blade – to mechanical energy, which later becomes electrical power with the help of the generator. The Figure 2.1 below show the critical parts of a HAWT as these components are described in [16].

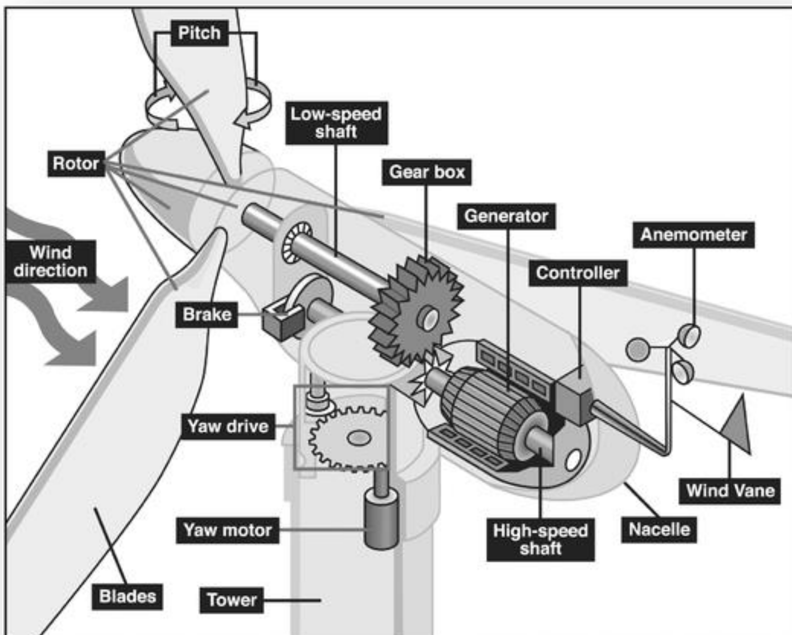

Figure 2.1 – Components of a three blades HAWT [17]

2.1.1. Tower

Tower is the structure that lifts up from the ground nacelle and the rotor. The height of the tower makes the rotor's blades work safe without touching the ground. Also, because the speed of the wind increases with the height above the earth allows taller WTGs to work in more efficient way and produce more energy.

2.1.2. Rotor

The blades and the hub together are called rotor. The blades are interacting with the incoming wind and due to their shape they create a lift force that makes them to rotate as it is shown in Figure 2.2 below.

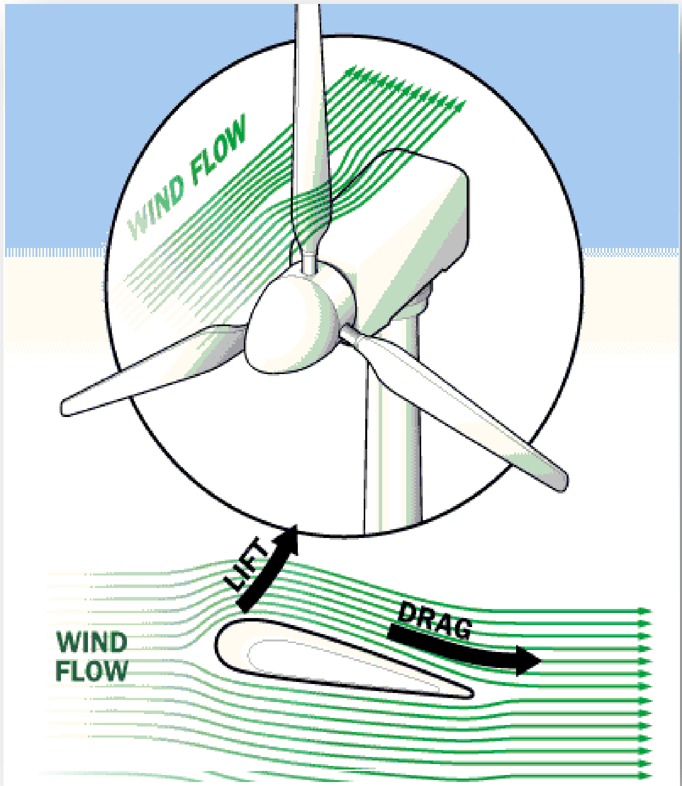

Figure 2.2 – Wind and blade interaction that creates the lift force and eventually the rotation of the blades [18].

The blades are attached – as it is shown in Figures 2.1, 2.2 – to the low-speed shaft in the hub, which turns at the same speed as the rotor. The hub is also consisted from the pitch mechanism. The pitch mechanism can regulate the angle of the blade, by the side or away from the incoming wind in order to make the rotor of the WT rotate faster or slower.

2.1.3. Anemometer & wind vane

Anemometer is a device that measures the wind and provides the recorded data to the WT controller. Commonly, the anemometer is placed in the back side of the nacelle as the following figure shows. The wind vane is used to orient the WTG against the wind. This vane determines the direction of the upcoming wind and delivers the information to the appropriate mechanism in order to turn (or not) the WTG.

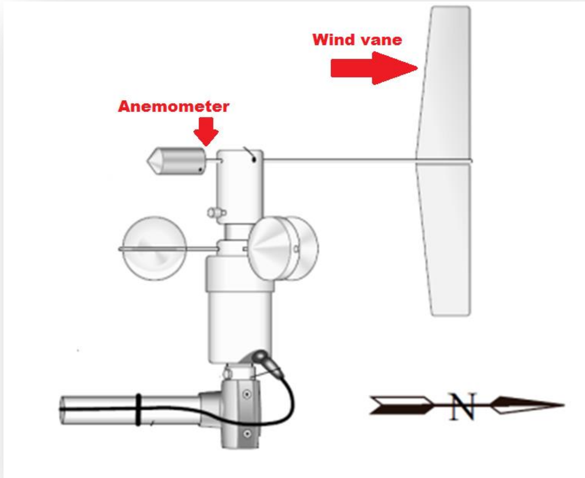

Figure 2.3 – Anemometer and wind vane as they are installed in a WTG [19].

2.1.4. Yaw mechanism

The yaw mechanism is a mechanical tool that turns the whole nacelle until it is oriented in such a manner that the rotor disc is perpendicular to the wind. All the HAWT tend to use a forced yawing that is a system consisting of electrical motors and gear boxes in order to keep the WT in the appropriate position, which is given through a controller from the wind vane [20].

2.1.5. Low-speed shaft

The low-speed shaft is the mean that transmits the rotational speed of the rotor to the gear box. The speed of the low-speed shaft is the same with the speed of the rotor.

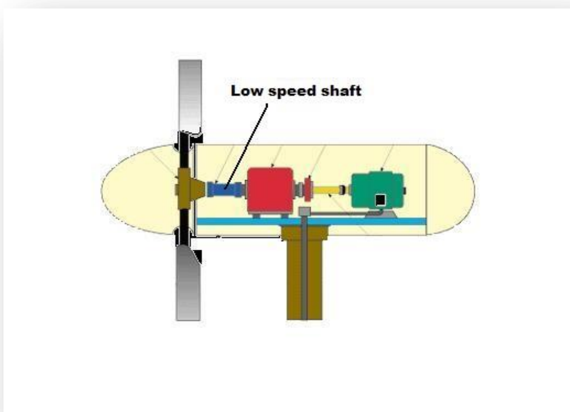

Figure 2.4 – Position of low-speed shaft in a WTG [21].

2.1.6. Gear box

The gear box is the connection between the low-speed and the high speed shafts. The actual performance that the gear box does is to increase the slow rotational speed (but higher torque) in order to get higher rotational speed (and eventually lower torque) to the generator.

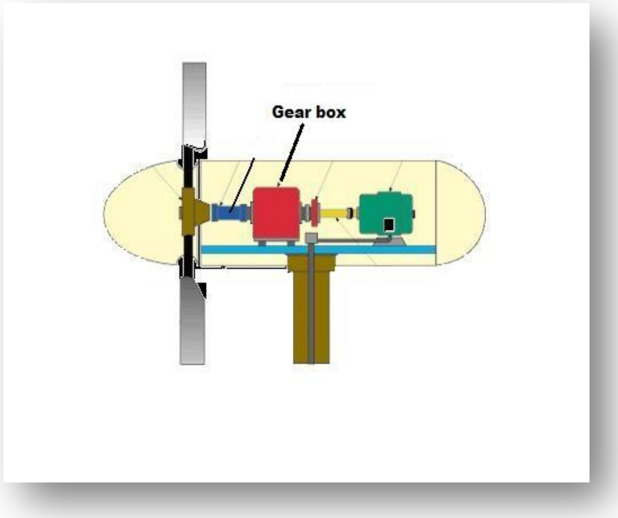

Figure 2.5 – Position of the gear box inside a WT [22].

2.1.7. High-speed shaft

High-speed shaft is the shaft transfers the high rotational speed into the generator. In reality is the connection between the gear box and the generator as it shown in the figure below.

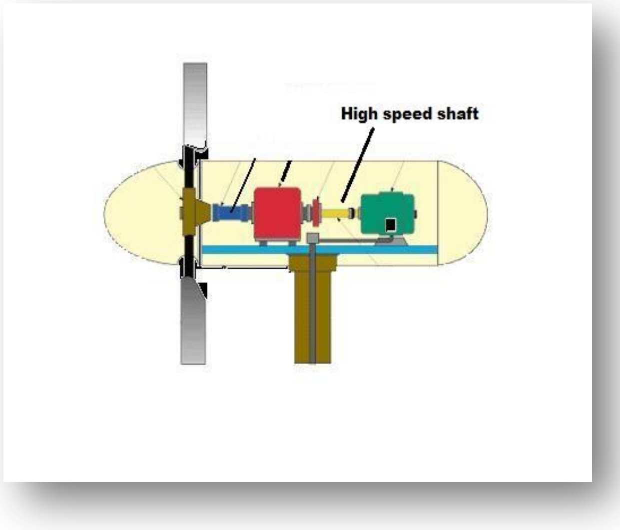

Figure 2.6 – The position of the high-speed shaft in the WT [22].

2.1.8. Generator

The WT's generator converts the incoming from the shafts, mechanical (rotational speed) energy into electrical power. The generators that the WTs are using are not close the regular generators that we can meet in the grid lines. This happens because these generators have to work with a power source – WT rotor – which provides a very fluctuating mechanical torque. Important parameters of the WT generator are the generating voltage, the cooling system and the switchers that start and stop the generator [20].

2.1.9. Brake

The mechanical brake of the wind turbine is used when a fail occurs or when the WTG has to be serviced. When is activated it ensures that the rotor will not rotate. Commonly is placed after the gear box.

2.2.LIDAR system

Usually in the industry, the estimation of the rotor's average wind speed is happening either from the measured rotor speed or from the anemometer that is mounted on the top of the nacelle (see Ch. 2.1.3) [21]. But these means are not very reliable sources because it is placed in the wake side of the rotor disc and often the measurements aren't precise, leading in approximations. Also, there is always a delay between the gatherings of the information from these systems that is bigger than the new technologies that are applied nowadays

This disadvantage of the anemometer can be eliminated with the use of a LIDAR device that can be placed in several places on the WT. Commonly is placed in the top of the nacelle as it is shown in Figure 2.7 below

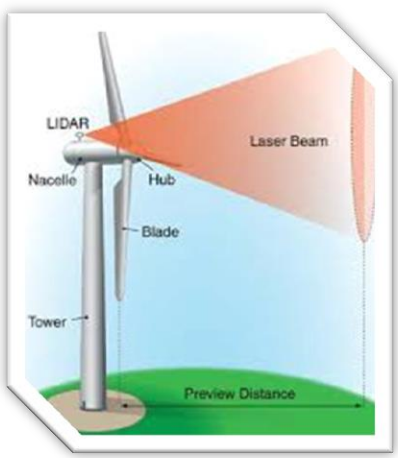

Figure 2.7 – Nacelle-mounted LIDAR, scanning in cone shape [23].

The device can be placed inside a wind farm as well as in offshore wind farms. As long as the LIDAR is facing and measuring the upcoming wind, is giving continuously useful data about the wind profile (direction, speed, turbulence etc.)

2.3. Wind turbine general control strategy

Generally, the ultimate goal of a WTG is to produce maximum power and so it is for its controller. In this subchapter we will describe how the controller of a WTG will maximize the produced power (power output).

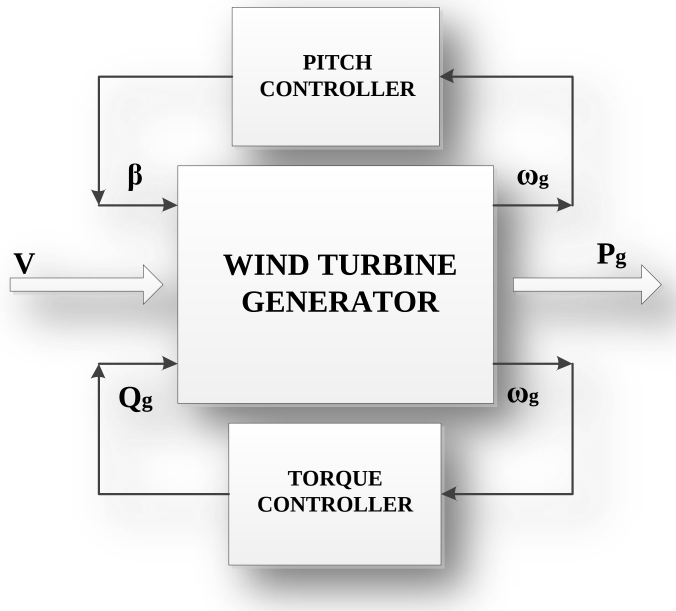

Figure 2.8 – General controller set up of a WTG with two controllers.

The figure above illustrates the block diagram model of general design for controlling the produced power of a WTG. It owes two controllers, the torque, T_g and the pitch, β controller. The load of the generated power is determined by the generated torque, T_g and the rotational speed of the generator, ω_g. The basic principal of a torque controller says that by controlling the generator's speed (ω_g) and by regulating the generator's torque (T_g), the generator of the WT will produce the maximum of its power. When the incoming wind (V) starts to rising, the torque controller will rise the load of the on the generator's side as well in order to maintain the produced power at maximum, until the loads of the generator and the rotor's speed reach the their limits for the WT. When the incoming wind speed (V) increases up to the rated value for the WT, the pitch controller embrace the torque controller. Then it adjusts the pitch angle, β, in order to extract less energy and the rotational speed is kept at the rated level.

Based on the above description and considering the controller's main target (maintain maximum power production), the values of the crucial parameters in reaction with the incoming wind are illustrating in the Figures below.

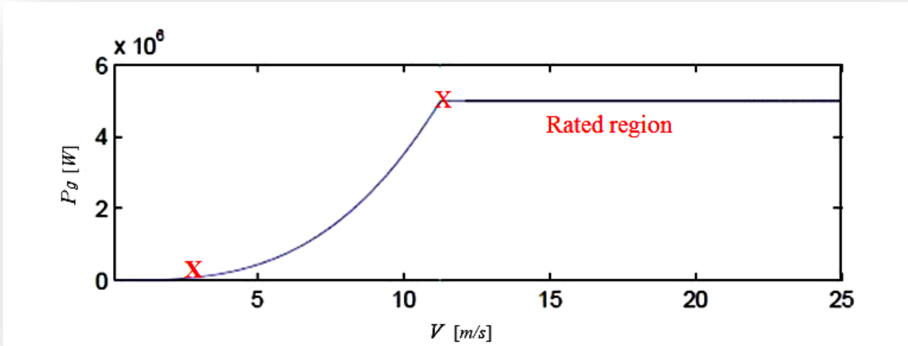

Figure 2.9 – Produced power vs. incoming wind relation based on values of the NREL 5MW WTG [16].

As we can see in Figure 2.9, we can separate the operation of the WT into three regions. Cut in speed region – 3m/s, first mark in the graph – where the turbine starts to produce power and increasing its production until the wind reaches the rated speed – second mark, 11,6m/s. After this spot the controller try to maintain into the limits of the produced power as it is explained before. Between the marks in the graph, the torque controller tries to regulate the produced torque, see figure below. This happens because it tries to keep the proportionality between the rotational speed and the rising wind speed as it Figure 2.9 shows, resulting in the maximizing of the produced power by the WTG.

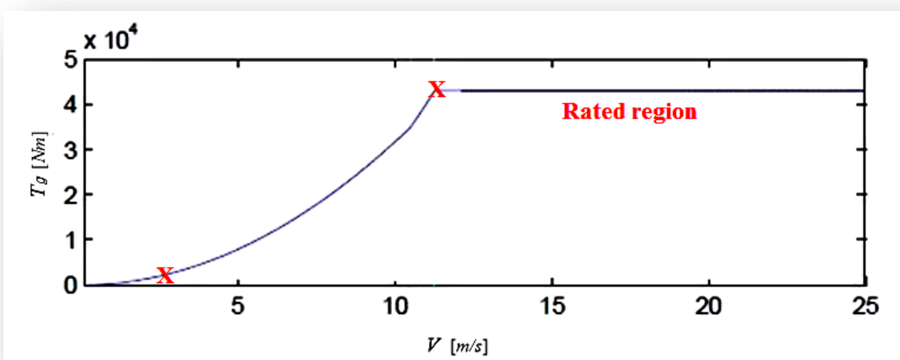

Figure 2.10 – Generated torque vs. incoming wind relation [16].

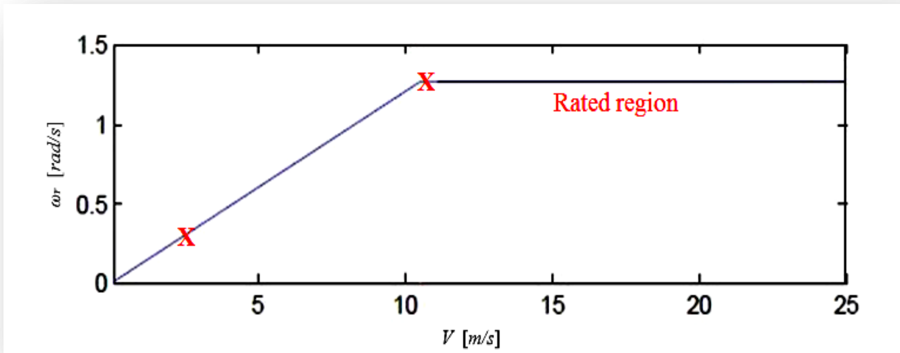

Figure 2.11 – Rotational speed vs. incoming wind relation [16].

As the wind speed keeps increasing, the value of wind is inserting in the last region – velocity bigger than the rated 11.4m/s – approaching the cut out value of 25m/s, where the operation of the WT stops. In this region the pitch controller takes charge and increases the value of the pitch angle in order to reduce the amount of the produced energy from the incoming wind and keep the produced power (P_g), the rotational speed (ω_g) and the generated torque (T_g) stable at the rated levels. How the pitch angle evolves through the transaction is illustrated in Figure 2.12 below.

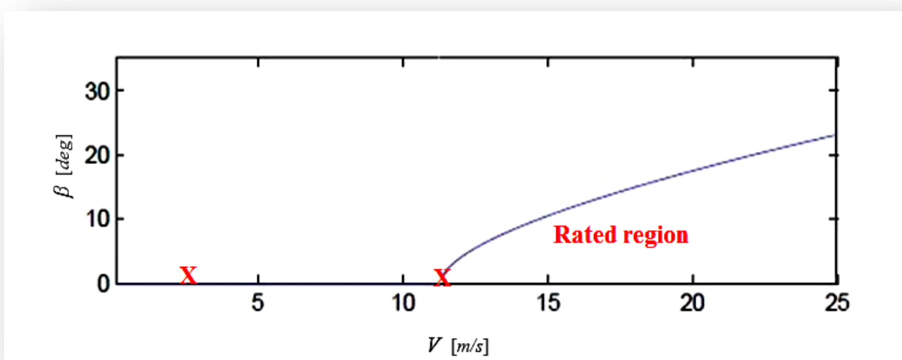

Figure 2.12 – Pitch angle vs. incoming wind relation [16].

Based on this strategy, which is widely used in the industry, the WTG will produce maximum power for wind with values until the rated one and will maintain constant power output for values higher than the rated wind speed. The values in the figure above are plotted based on the proposed 5MW wind turbine [16].

2.4.CVXGEN [24]

CVXGEN is an online code generator for convex optimization. This tool is essential for our control strategy because it will generate and operate as the optimization solver for our designed MPC. The use was under a student license kindly given by the authors of the program.

This tool generates by its own a code, in C language, for solving quadratic problems represented as convex optimization ones. It uses an online interface with no specific needs for software installations and solves the given mathematical problems fast, accurate and in minimal cost effort – something really important for the control industry, when it is operating online.

As input, CVXGEN needs from the user to describe the quadratic problem in simple language. Then automatically creates free to manipulate, libraries in C code for custom, high speed solver. Afterwards, this can be downloaded and used directly, without the use of a compiler or something similar. The main advantage is that CVXGEN is compatible with Matlab functions that with simple command, downloads and builds in Matlab a mex solver ready to use. We choose to use this solver because it can solve problem up to 10.000 times faster (for simple problems) and for its compatibility with Matlab/Simulink. The limitation of the program is that CVXGEN solves QP representable problems only. Also it works in full potential for problems where the final plant has less the 2000 coefficients in the constraints and objective sections.

When the program is ready, it can co-operate with Simulink with the help of an S Function block. Then the S-Function operates as our “custom” model predictive controller as optimizes and gives the control signal based in our requirements.

3. MODELING OF THE SYSTEM

In order to design an advance controller and conduct simulations, a linear model of the turbine needs to be derived. This is because the controllers that we will use in later stages are linear model based controller, meaning that they need the actual linear model of the system and not an identified one or similar. The derived model is similar to known models, based on the components that we described in the previous chapter, which can be found around the literature and scientific reports. The modeling of the WT occurred based on [10, 11, 15, 16, and 27]

3.1. Approaching the model

For the WT, a nonlinear model is defined. All the parts of the plant are derived based on the understanding of the physical laws and the governing equations that work around a WT. This method is used instead of, for example system identification method, because in this way gives better understanding and representation of the working principles of the turbine operation. This help in the design, construction and analysis of the controller in the later stages as well.

On one hand, based on its physical behavior, a WT model is a non-linear plant model. This is acceptable and it is used to run simulations for the WT. On the other hand, in order to design a controller for the plant, a linear model of the turbine is needed. This happens because most of the controllers – and the one that considered in this project – are linear.

The main target of this project is to design a model predictive controller that will be able to control the deviations that occur, due to disturbance, at the system's states and drive the WT away from its steady state position. This position is defined by the linearization point that will be in the rated region (see Ch. 2.3). The defined model of the plant will reflect in this sense. Also, the output of the systenm should be able to play key role in the energy production, as the main goal of controller is the power production and the increase of the WT operational lifetime.

In order to test the defined, linear and non-linear model, they have been simulated with different inputs of the wind (disturbance) in the region where the WT operates with rated values for the pitch angle and the rotor speed. If the controller works well enough in this region an attempt to other region will be conducted as well. Good results meaning that the model behaves as it expected under the inputs and always based on the physical laws that working in a real WT.

3.2.General model of a wind turbine

Before define the model, the need of analyzing and understanding the working principle of a WT model is needed. A general model is divided in several sub-models and analyzed separately. Then, based on this model and its behavior, the constructed model will be introduced and derived as well. As the figure below shows, the model of the wind is considered as external and not analyzed in this project. It is only explained briefly.

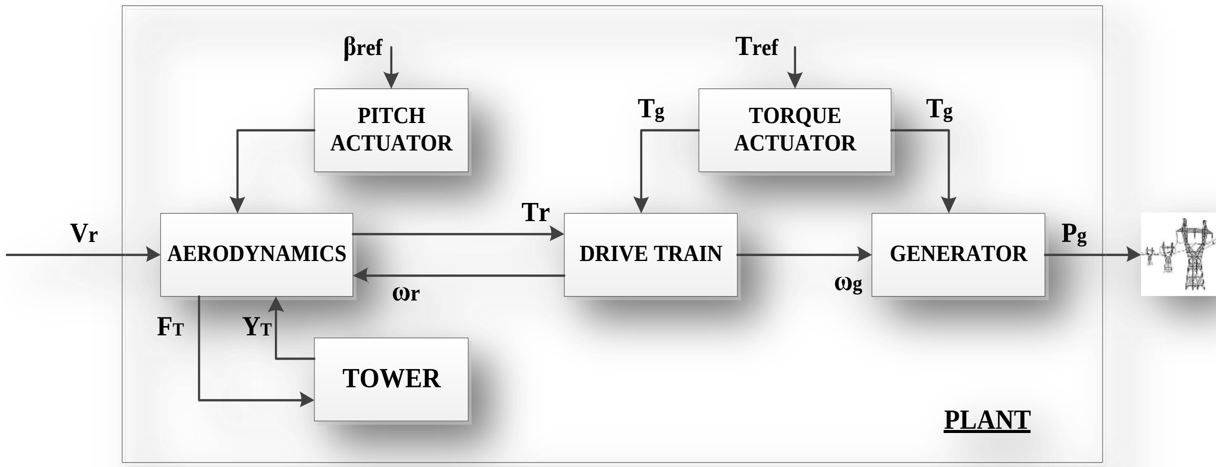

Figure 3.1 – Block diagram of the sub-models that establish the WT/plant model.

The inputs for this – Figure 3.1 – system are the controllable inputs pitch angle, β, and the generators' torque, T_g and the output of the system is the produced by the generator power, P_g.

In order to derive the model, some simplifications were made. These are addressed here for better understanding of the upcoming modelling procedure.

1. *Wind*: the model of the wind is described but not modelled. Since the wind is chaotic in the nature is also very complicated for modelling. Additionally, in this thesis the wind is considered as known disturbance and since that was conceded as major factor of influence. Finally, the values of the wind that were used for the simulations and the creation of the controller were given based on the values that have been used in the model that this thesis' controller is compared to [16].
2. *Aerodynamics*: this sub-model of the WT is constructed according to the BEM theory. The main assumption there is the rigid blades and the collective pitch control that occurs in all of the blades at the same time.
3. *Drive Train*: the drive train of the plant was modelled as a rotating mechanical system that consists of a gear and a shaft on the rotors' side. This model takes the low speed/high torque from the rotors' side and translates it into high speed/low torque in the generators' side.
4. *Generator*: the generator describes how much electrical power is produced and the gives the torque load to the system.
5. *Tower*: this model shows the tower defection (back and forth) when the wind hits the tower. The tower is modelled as a single mass that is affected by a force produced by the rotor, the stiffness and the damping of the tower.
6. *Pitch & torque*: these actuators are modelled as simple 1st order systems.

3.3.Wind model description

For the completion of the thesis (due to time and complexity of the phenomenon) the model of the wind is not derived as we have the opportunity to use given values for the wind. Instead a brief explanation of the components of a possible wind model is given.

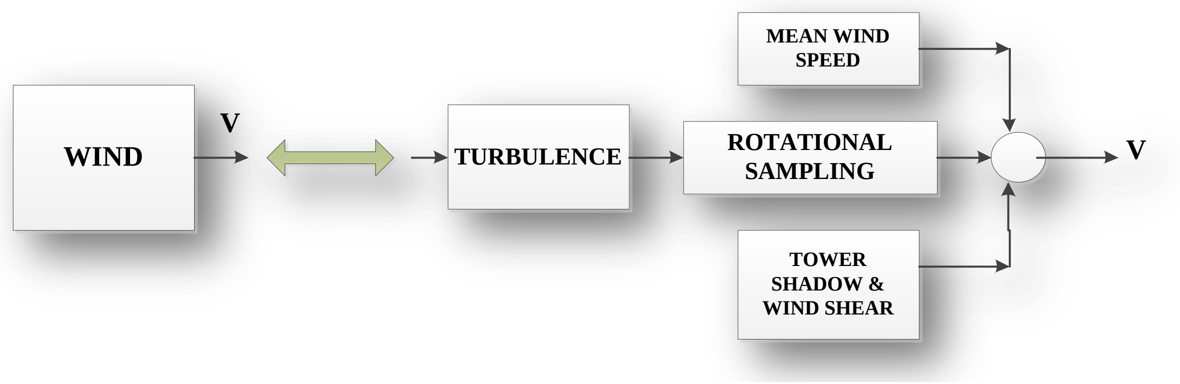

Figure 3.2 – Wind profile structure & components that establish it.

The wind is hard to modeled, as it varies over time and space. This gives a chaotic representation to it. The location of the installed WT on earth (offshore or onshore) and mostly the local geographical properties, have huge contribution in the development of the wind across a turbine. Additionally, the date of the year, due to commonly periodic effects (seasons with high intensity wind streams are very common in southern regions) can contribute positively or negatively to the weather and so on the wind development and wind changes across the installed WT [25]. For this project, only fast changes in the wind are considered and used.

As it can be seen in the Figure 3.2, the wind consists of five different parts that if we put them all together they create the average rotor wind speed as output. These are:

- Mean wind speed
- Turbulence
- Tower shadow
- Wind shear
- & Rotational sampling

The turbulence part is the fast changes of the wind and majorly are guided by the topography of the area (like mountains, fields etc.) and temperature variations which often affect the wind evolution. The modeling of the turbulence is a stochastic process.

Tower shadow part models the influence that the tower has to the wind speed. The blades of the WT are part of the tower, since the tower shadow models as well the influence on the blades when the wind speed pass through tower.

Wind shear part represents the friction between the ground and the air. This happens because the mean wind speed is higher over the ground. Thus, the mean wind is also higher for the blades that they are pointing upwards compare to the blades pointing downwards.

Lastly, the rotational sampling is a two filter model. A low pass filter to represent the fictitious wind speed, which actually is a scalar wind speed for the whole rotor plane. Then, the second filter works as extra filter that absorbs the rotation of the blades by the augmentation of their rotationally frequency.

For the simulations in Matlab & Simulink, the wind field averaged over the WT's rotor plane.

3.4.Aerodynamics model description

This sub-model shows how the wind interacts with the WT. The Figure 3.3 shows with which other sub-models the aerodynamics part interacts and which are the inputs and the outputs of it.

Firstly, the wind input, V that we described in Ch. 3.3 is the averaged wind speed that the entire rotor disc "sees". Continuously, it has the pitch angle, β, which describes the angle of the blades. The pitch system is described later briefly.

Additionally, as the figure below shows, there is interaction between the tower and the aerodynamics model through the tower fore-aft velocity, Y_T. For the aerodynamics model perspective, the tower fore-aft affects the wind speed that "hits" the rotor disc. For instance, when the tower oscillates into the wind, the wind speed that the rotor disc feels is higher than the actual/real wind speed. Oppositely, the wind speed is lower when the tower's oscillation direction is occurring with the wind direction. Also, in the figure we can see the force from the aerodynamics to the tower model, the thrust force F_T that is the generated from the wind that hits the rotor disc and tends to push it backwards and eventually leads the whole tower moving backwards.

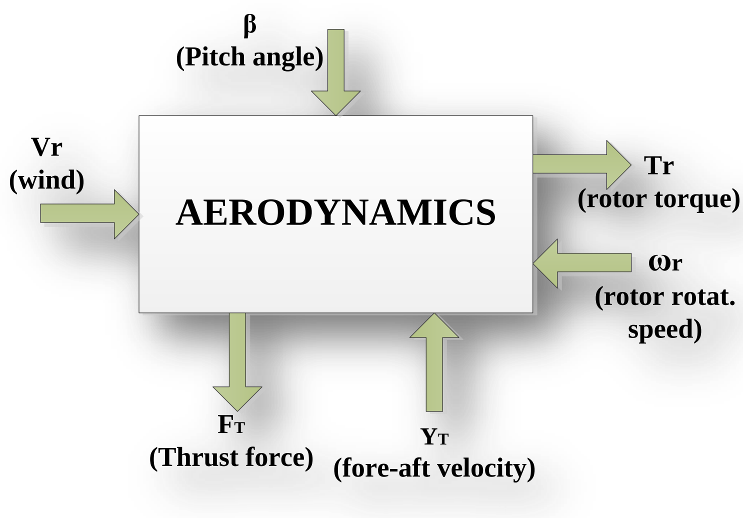

Figure 3.3 – Input and output signals for the aerodynamics part of the model plant.

Lastly, the interaction between the aerodynamics of the system and the drive train occurs. There it can be seen firstly the speed of the rotor, ω_r that is given by the drive train. This parameter is very important for a WT, because the amount of produced energy from the wind strictly depends on the ration between the rotor's speed (ω_r) and the winds' speed. Also this interaction includes the produced by the rotor disc torque, T_r and is the toque that the rotor gives to the drive train and eventually transferred to the generator.

3.4.1. About rotor disc

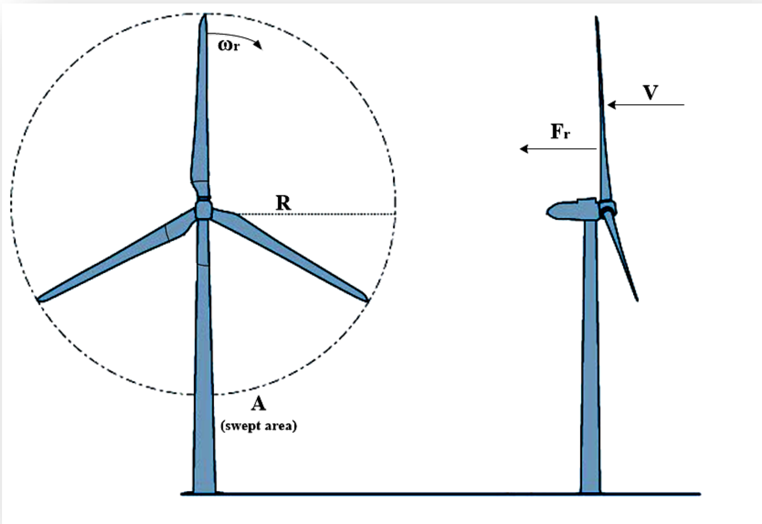

Figure 3.4 – Illustration of the rotor disc area and the parameters that are seen on it.

The Figure 3.4 shows a 3-blade WT. The so called rotor disc in the turbine is the disc that the blades create when they rotate (dashed line in the left side of the picture). The useful parameters that someone can observe are, ω_r the rotor's speed, R the rotor disc radius, A is the swept area that the rotor disc coves, V the wind that the rotor disc faces and finally F_T the force generated by the wind in the rotor disc.

3.4.2. The kinetic energy in the wind

Before defying the aerodynamic equation, it is needed to understand how the wind affects the WT and what kind of energy is carrying in it. As it is known, the wind before reaching the turbine it behaves as uniform air flowing in the direction of the wind. Thus the wind, V can be described as airflow with the mass flow rate calculated as:

$$\dot{m}_V = \rho A V \qquad \text{Eq. 3.1}$$

where ρ is the density of the air, A is the cross section of the area that the air flows (in our case is similar with the swept area,A).

Based on fluid dynamics theory, the force inside the wind, F_V can be expressed as:

$$F_V = \frac{1}{2}\dot{m}_V V = \frac{1}{2}\rho A V^2 \qquad \text{Eq. 3.2}$$

and then, based in Eq. 3.1 – 3.2 about the kinetic energy of the wind, that is the energy that actually rotates the WT's blades. The kinetic energy can be calculated as:

$$P_V = F_V V = \frac{1}{2}\rho A V^3 \qquad \text{Eq. 3.3}$$

These two parameters, F_V & P_V are the main dynamics that are used to model the aerodynamics part of a WT model.

3.4.3. Wind turbine & wind interaction

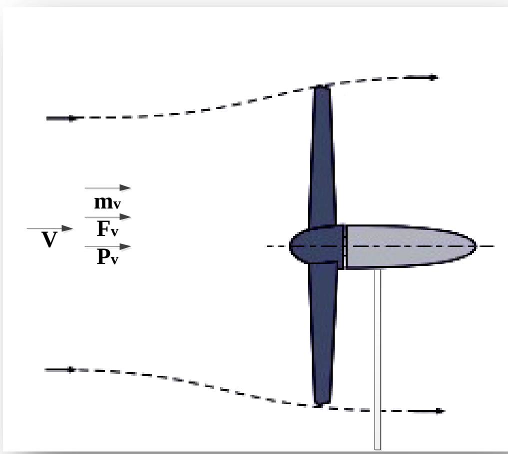

Figure 3.5 – The WT placed in front of the airflow.

When the wind flows through a WT, the turbine extracts energy from it and converts the kinetic energy of the wind into mechanical energy. Yet, not all the energy can be extracted, but only a part and this part can be calculated from the following:

$$P_r = P_V C_P \qquad \text{Eq. 3.4}$$

In Eq. 3.4, C_P is the known power coefficient and can be derived based on the actuator disc theory as it is described in [26]. This coefficient can be mainly explained by two simple things.

Firstly, when wind has a drop in its speed, as it flows through the rotor disc, but the mass flow ($\dot{m}_V$) has to be the same in both sides of the rotor disc. In Eq. 3.1, the cross section area, A, has to grow as the wind dashes down, which introduces the impression that the air flow is not anymore uniform, as it is shown in Figure 3.5. The figure shows that the cross section area where the wind in free stream can flow is small compare to the rotor area that is bigger. This is why it is introduced to the WT the known Betz limit (0.593), which actually is the maximum value that C_P can obtain. Also, the other thing that affects the C_P value is the aerodynamics part of the rotor disc.

For better understanding and notation issues (for use it in later stages) is safe to define now the tip-speed ratio, λ, that contributes to the C_P calculations (in this thesis the power coefficient values are based on a look-up table that consists values of λ-tip speed ratio & β-pitch angle). The tip speed ratio is calculated as the results of ratio between the rotor's, ω_r, and the wind speed, V:

$$\lambda = \frac{\omega_r R}{V} \qquad \text{Eq. 3.5}$$

Figure 3.6 shows the different values of the power coefficient for different values of λ and β, which also show the non-linear form of the aerodynamics model. The values for these properties are taken from the [16] and it shows that the maximum value of C_P is smaller than the Betz limit that we mentioned before.

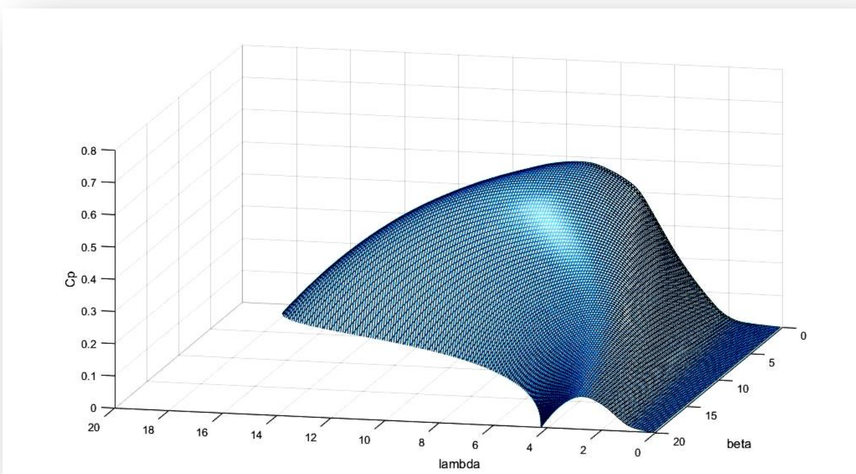

Figure 3.6 – Power coefficient (Cp) and its nonlinear connection with the tip speed ratio and the pitch angle [16].

Based on the previous explained equation (Eq. 3.1-3.5) and replacing the swept area, A with πR^2 we can calculate the rotor disc produced power as:

$$P_r = \frac{1}{2}\pi\rho R^2 V^3 C_P(\lambda,\beta) \qquad \text{Eq. 3.6}$$

Then the output of the aerodynamics model, the torque generated by the rotor, it can be calculated as:

$$T_r = \frac{P_r}{\omega_r} \qquad \text{Eq. 3.7}$$

re-write in its next form by inserting Eq. 3.6 and we result in:

$$T_r = \frac{1}{2\omega_r}\pi\rho R^2 V^3 C_P(\lambda,\beta) \qquad \text{Eq. 3.8}$$

Similar with the torque the thrust force is calculated. In this case, we don't use C_P but a similar coefficient, the thrust coefficient C_T. This coefficient measures how much of the force of the wind can be applied to the rotor disc. This thrust force is given as:

$$F_T = F_V C_T \qquad \text{Eq. 3.9}$$

By combining Eq. 3.2 and Eq. 3.9 will result the final form of F_T:

$$F_T = \frac{1}{2}\pi\rho R^2 V^2 C_T(\lambda,\beta) \qquad \text{Eq. 3.10}$$

The wind which the rotor disc "sees" is affected by the tower movement as we saw before. In order to be more precise we need to include the tower movement in the aerodynamics model and finally replace the wind, V with the new more precise variable. This is calculated as:

$$V_r = V - \dot{Y}_T \qquad \text{Eq. 3.11}$$

where, V_r is the related wind speed that the rotor disc $\dot{Y}_T$ is the tower speed fore-aft. Based on this change we can re-write in their final form our outputs of the model as they are shown below:

$$T_r = \frac{1}{2\omega_r}\pi\rho R^2 {V_r}^3 C_P(\lambda,\beta) \qquad \text{Eq. 3.12}$$

$$F_r = \frac{1}{2}\pi\rho R^2 {V_r}^2 C_T(\lambda,\beta) \qquad \text{Eq. 3.13}$$

3.4.4. State space representation

In order to able to linearize these two parameters we will use a 1st order Taylor series expansion at specific operating point. The determination of the operating point is depending on the values of ω_r, V_r, and β firstly and subsequently C_p and λ. From now and on these operating points are denoted as ω_{r0}, V_{r0}, C_{P0}, λ_0 and β_0.

Then Eq. 3.12 can be expressed as:

$$T_{r0} = \frac{1}{2\omega_{r0}}\pi\rho R^2 {V_{r0}}^3 C_{P0}(\lambda_0, \beta_0) \quad \text{Eq. 3.14}$$

The Taylor expansion results a small signal in order to be able and compensate when the model deviates away from the operating point. These deviations are denoted as ex. $\Delta\omega_r=\omega_r- \omega_{r0}$. Then the rotor torque is expressed as:

$$T_r = T_{r0} + \frac{\partial T_r}{\partial \omega_r}\Big|\omega_{r0} \cdot \Delta\omega_r + \frac{\partial T_r}{\partial V_r}\Big|V_{r0} \cdot \Delta V_r + \frac{\partial T_r}{\partial \beta}\Big|\beta_0 \cdot \Delta\beta \quad \text{Eq. 3.15}$$

Assuming that T_{r0} is very small we consider it as zero and then Eq. 3.15 can be re-written in state space form as:

$$\Delta T_r = \left[\frac{\partial T_r}{\partial \omega_r}\Big|\omega_{r0} \;\; \frac{\partial T_r}{\partial V_r}\Big|V_{r0} \;\; \frac{\partial T_r}{\partial \beta}\Big|\beta_0\right]\begin{bmatrix}\Delta\omega_r \\ \Delta V_r \\ \Delta\beta\end{bmatrix}$$

Where:

$$\frac{\partial T_r}{\partial \omega_r}\Big|\omega_{r0} = \frac{1}{2}\pi\rho R^2 {V_{r0}}^3\left(-\frac{1}{{\omega_{r0}}^2}C_{P0} + \frac{1}{\omega_{r0}}\frac{R}{V_{r0}}\frac{\partial C_P(\lambda_0,\beta_0)}{\partial \lambda_0}\right)$$

$$\frac{\partial T_r}{\partial V_r}\Big|V_{r0} = \frac{1}{2\omega_{r0}}\pi\rho R^2\left(3{V_{r0}}^2 C_{P0} - {V_{r0}}^2\lambda_0\frac{\partial C_P(\lambda_0,\beta_0)}{\partial \lambda_0}\right)$$

$$\frac{\partial T_r}{\partial \beta}\Big|\beta_0 = \frac{1}{2\omega_{r0}}\pi\rho R^2 {V_{r0}}^3\left(\frac{\partial C_P(\lambda_0,\beta_0)}{\partial \beta_0}\right)$$

Useful for these transformations was the Eq. 3.5 derivatives as:

$$\frac{\partial \lambda}{\partial \omega_r}\Big|\omega_{r0} = -\frac{R}{V_{r0}} \quad \text{and} \quad \frac{\partial \lambda}{\partial V_r}\Big|V_{r0} = -\frac{\omega_{r0}R}{{V_{r0}}^2}$$

These two equations help to simplify the previous equations.

The same procedure was followed for the thrust force as well and Eq. 3.12 expressed as:

$$F_{T0} = \frac{1}{2}\pi\rho R^2 {V_{r0}}^2 C_{T0}(\lambda_0, \beta_0) \quad \text{Eq. 3.16}$$

and in Taylor series expansion form as:

$$F_T = F_{T0} + \frac{\partial F_T}{\partial \omega_r}\Big|_{\omega_{r0}} \cdot \Delta\omega_r + \frac{\partial F_T}{\partial V_r}\Big|_{V_{r0}} \cdot \Delta V_r + \frac{\partial F_T}{\partial \beta}\Big|_{\beta_0} \cdot \Delta\beta \qquad \text{Eq. 3.17}$$

Assuming again that F_{r0} is very small we consider it as zero and then Eq. 3.15 can be re-written in state space form as:

$$\Delta F_T = \begin{bmatrix} \frac{\partial F_T}{\partial \omega_r}\Big|_{\omega_{r0}} & \frac{\partial F_T}{\partial V_r}\Big|_{V_{r0}} & \frac{\partial F_T}{\partial \beta}\Big|_{\beta_0} \end{bmatrix} \begin{bmatrix} \Delta\omega_r \\ \Delta V_r \\ \Delta\beta \end{bmatrix}$$

Where:

$$\frac{\partial F_T}{\partial \omega_r}\Big|_{\omega_{r0}} = \frac{1}{2}\pi\rho R^3 V_{r0} \frac{\partial C_T(\lambda_0, \beta_0)}{\partial \lambda_0}$$

$$\frac{\partial F_T}{\partial V_r}\Big|_{V_{r0}} = \pi\rho R V_{r0} C_{T0} - \frac{1}{2}\pi\rho R^3 \omega_{r0} \frac{\partial C_T(\lambda_0, \beta_0)}{\partial \lambda_0}$$

$$\frac{\partial F_T}{\partial \beta}\Big|_{V_{r0}} = \frac{1}{2}\pi\rho R^2 {V_{r0}}^2 \frac{\partial C_T(\lambda_0, \beta_0)}{\partial \beta_0}$$

3.5.Drive train model description

This part describes the mean which transfers the rotor torque that is produced by the incoming wind into the generator part of the WT. The drive train model consists of the following parts that also the Figure below.

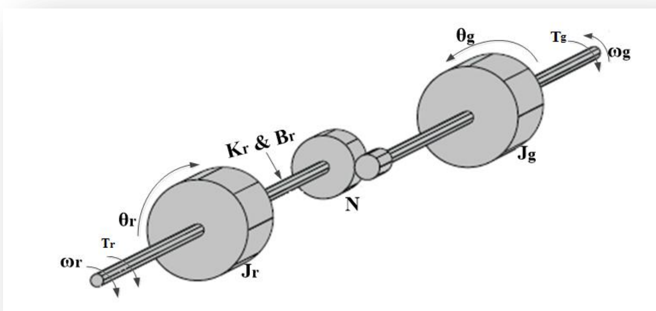

Figure 3.7 – Free body diagram of drive train of a WT.

The inertia of the rotor, Jr and the inertia of the generator, Jg, are included as well. In the interval of the inertias there is a gearing that transforms the energy with ratio N. The shaft between the gearbox and the drive train is flexible and represented with the use of torsion stiffness K_r and a damping B_r. The shaft on the other side assumed to be rigid. The derivation of the two inertias is happening separately and then included in the full drive train model. This helps also in understanding and shows that the model does not include nonlinearities.

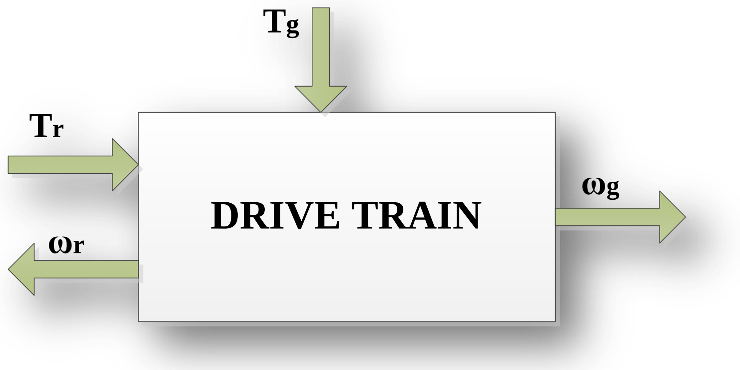

Figure 3.8 – Drive train block with inputs and outputs of the model.

The rotor side of the drive train (low speed shaft) gives the following equation for the modeling of the drive train:

$$J_r\dot{\omega}_r = T_r - K_r\,\theta_t - B_r(\omega_r - \frac{\omega_g}{N}) \qquad \text{Eq.3.18}$$

where the positive direction is based on the rotor torque (T_r) and θ_t represents the torsion that occurs in the shaft. This torsion is given as:

$$\theta_t = \theta_r - \frac{\theta_g}{N} \qquad \text{Eq. 3.19}$$

In this approach of the modeling torsion only torsion is in our interest and we have no need of angles in the drive train, thus we can introduce that $\dot{\theta}_t = \omega$ that leads us to the conclusion that the changes in the torsion can be shown as:

$$\dot{\theta}_t = (\omega_r - \frac{\omega_g}{N}) \qquad \text{Eq. 3.20}$$

Based on similar analysis we can model the inertia in the generator side (high speed shaft) but this time the rotational speed (ω_g) gives the positive direction, oppositely from the torque (T_g).

$$J_g\dot{\omega}_g = -T_g + \frac{1}{N}K_r\,\theta_t + \frac{1}{N}B_r(\omega_r - \frac{\omega_g}{N}) \qquad \text{Eq. 3.21}$$

3.5.1. State space representation

The Eq. 3.18, 3.20 & 3.21 are first order differential equations. They can be expressed in linear state space equation for as it follows:

$$\begin{bmatrix}\dot{\omega}_r\\ \dot{\omega}_g\\ \dot{\theta}_t\end{bmatrix} = \begin{bmatrix} -\frac{B_r}{J_r} & \frac{B_r}{NJ_r} & -\frac{K_r}{J_r}\\ \frac{B_r}{NJ_g} & -\frac{B_r}{N^2J_g} & \frac{K_r}{NJ_g}\\ 1 & -\frac{1}{N} & 0\end{bmatrix}\begin{bmatrix}\omega_r\\ \omega_g\\ \theta_t\end{bmatrix} + \begin{bmatrix}\frac{1}{J_r} & 0\\ 0 & \frac{1}{J_g}\\ 0 & 0\end{bmatrix}\begin{bmatrix}T_r\\ T_g\end{bmatrix} \qquad \text{Eq. 3.22}$$

This drive train model results the needed for the WT model outputs and is linear as well.

3.6. Generator & Torque actuator models description

The generator is the part of the WT that transforms the mechanical torque that the drive train provides into power.

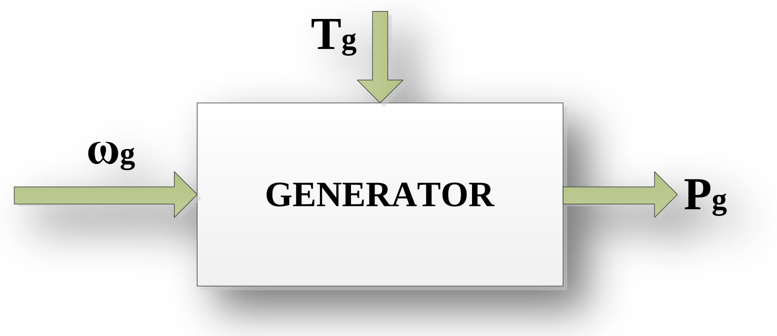

Figure 3.9 – Generator model block with inputs torque and rotational speed and power as output.

As the figure above shows, the inputs of the generator are the incoming from the drive train rotation speed, ω_g and the given generator torque load T_g. As result we have the produced power, P_g in the output. Here is safe to mention that the output of the generator is not used directly in the designing of the controller but is considered as output of the WT model for analysis purposes. The generator has a non-linear model.

As the rotational energy is converted to electrical power some of the energy is becoming losses through the convention but it can be assumed a loss-less generator model. Then, the total amount of extracted energy is given by the following equation:

$$P_g = \omega_g T_g \qquad \text{Eq. 3.23}$$

Also we can say that the T_g is controllable variable depending on the electrical load of the generator.

In the generator model, the torque actuator is having a crucial role because is feeding the generator with the needed electrical load in order to control it. In real situations, generators cannot change their load instantly. Therefore the torque actuator is represented by a first order model with form:

$$\dot{T}_g = -\frac{1}{\tau_g} T_g + \frac{1}{\tau_g} T_{g,ref} \qquad \text{Eq. 3.24}$$

Where τ_g is the generator's time constant and $T_{g,ref}$ is the desired torque and is equal with the referenced power divided by the rotational speed of the generator ($\frac{P_{ref}}{\omega_g}$). These approaches of the equations leave the generator with a non-linear model.

3.6.1. State space representation

Before defining the state space equations we linearize again the generator model. We are doing this under the same principle that we linearized the previous models (Taylor expansion approximation). It was linearized around the operating point of P_{g0} and then Eq. 3.23 looks like:

$$P_g = P_{g0} + \frac{\partial P_g}{\partial \omega_g} \Big| \omega_{g0} \cdot \Delta\omega_g + \frac{\partial P_g}{\partial T_g} \Big| T_{g0} \cdot \Delta T_g \qquad \text{Eq. 3.25}$$

Where:

$$\frac{\partial P_g}{\partial \omega_g} \Big| \omega_{g0} = T_{g0} \ \& \ \frac{\partial P_g}{\partial T_g} \Big| T_{g0} = \omega_{g0}$$

3.7.Tower model description

This model describes the movement of the tower when the wind hits the rotor, which continuously affects the wind speed that the rotor can see. The tower model is affected and affects directly only with the aerodynamic model and as we can see in the following figure the input of it is the thrust force, F_T and the output of it is the fore-aft movement of the tower, $\dot{Y}_T$. This parameter, the fore-aft movement is the one of the parameters that affects the wind speed seen by the rotor of the WT.

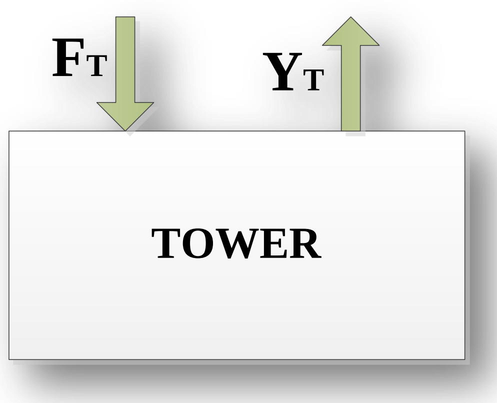

Figure 3.10 – Tower block with inputs and outputs.

The wind will move back the WT with force (F_T) and eventually will make the nacelle push back and front. This happens because the tower's stiffness gives a proportionality to the displacement force ($\dot{Y}_T$), but in the opposite direction.

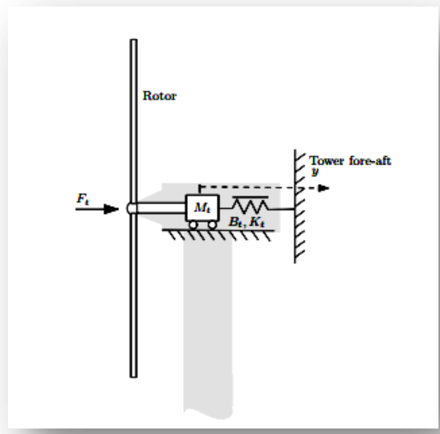

Figure 3.11 – Mechanical representation of the tower's acting forces [27].

Additionally, the tower is a light damp structure (metallic structure of huge size). Based on the Figure 3.11 above and the free body diagram below we can easily simplify the model into a simple second order, mass-spring-damp model.

Figure 3.12 – representation of the tower in free body diagram and the dynamics acting on it.

The dynamics have the form:

$$m_T \ddot{Y}_T = F_T - K_T Y_T - B_T \dot{Y}_T \quad \text{Eq.3.26}$$

Where the force of the aerodynamics (F_T) define which direction is considered as positive and m_T is the modal mass for the tower of the WT.

3.7.1. State space representation

This model has no need for linearization, so we directly transform it the state space form that looks like:

$$\begin{bmatrix} \dot{Y}_T \\ \ddot{Y}_T \end{bmatrix} = \begin{bmatrix} 0 & 1 \\ -\frac{K_T}{m_T} & -\frac{B_T}{m_T} \end{bmatrix} \begin{bmatrix} Y_T \\ \dot{Y}_T \end{bmatrix} + \begin{bmatrix} 0 \\ \frac{1}{m_T} \end{bmatrix} [F_T] \qquad \text{Eq. 3.27}$$

3.8.Pitch actuator model description

The pitch actuator, like the torque one is one of the control inputs of the system. In this case the pitch actuator is relative slower than the torque one and again the model of it is expressed by a first order system with a time constant, τ_p as it is shown below:

$$\dot{\beta} = -\frac{1}{\tau_p}\beta + \frac{1}{\tau_p}\beta_{ref} \qquad \text{Eq. 3.28}$$

3.8.1. State space representation

For both actuator models (pitch & torque as well) the state space look like:

$$\begin{bmatrix} \dot{\beta} \\ \dot{T}_g \end{bmatrix} = \begin{bmatrix} -\frac{1}{\tau_p} & 0 \\ 0 & -\frac{1}{\tau_g} \end{bmatrix} \begin{bmatrix} \beta \\ T_g \end{bmatrix} + \begin{bmatrix} \frac{1}{\tau_p} & 0 \\ 0 & \frac{1}{\tau_g} \end{bmatrix} \begin{bmatrix} \beta_{reg} \\ T_{g,ref} \end{bmatrix} \qquad \text{Eq. 3.29}$$

3.9.Model definition and verification

All the previous (Eq.3.1 -3.29) equations can construct and replicate the dynamics of a wind turbine model. The dynamics of the WT will be modeled using a simplified version of this model including aerodynamics part and drivetrain as well. For controlling issues it is observable that key parts in the whole WT operation is the rotor's speed (ω_r), the pitch angel (β) and the effect that the wind (V_r) has to it. Therefore the system is modelled with respect to these values

3.9.1. The nonlinear model validation

Assuming that the drive train is rigid we can express the rotor's speed, based on the Eq. 3.12, 3.18 & 3.23 as:

$$J_{tot}\dot{\omega}_r = T_r - NT_g \qquad \text{Eq. 3.30}$$

where, the $\dot{\omega}_r$ depends on the generator's torque and the rotor's torque respectively. For the model creation in Simulink the reference power that is included in the generator's torque assume to be constant and it value at 5MW.

In order to replicate the behavior of the proposed model we construct in Simulink a nonlinear model based on the Eq. 3.30. Simulating both nonlinear and NREL model it can be concluded that the defined one behaves as the actual one in the operating point, V_{op}=18m/s. The following graph validates the claim that the models fit at the rated region (Region 3, Ch. 2.3).

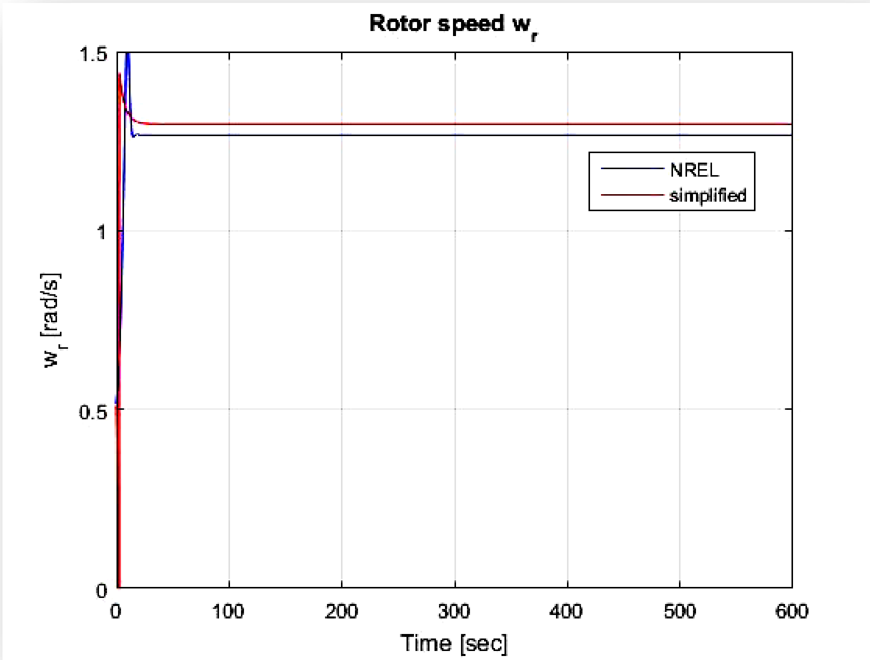

Figure 3.14 – NREL 5MW vs. designed non-linear model behavior in constant wind speed of 18m/s.

As it is observable, both systems have a small increase in the beginning due to the instant increase in the wind velocity and then start working in their rated values for ω_r (nonlinear ω_r=1.28 rad/s and linear ω_r=1.298 rad/s). During this procedure the input for the system, the pitch angle was constant in the nominal region of 14.89^o.

For Simulink schemes for both nonlinear plants look Appendix Part A.

In order to linearize the Eq. 3.30 through Taylor series expansion around equilibrium points (V_{r0}, ω_{r0} & β_0), we assume that $T_r|_{o.p.} = NT_g|_{o.p.}$ and J_T the total inertia on the both side of the drive train shaft. Then Eq. 3.30 transforms into the following equation, which from now and on will represent the deviations away from the equilibrium points and has the form:

$$\Delta\omega_r = \frac{1}{J_T}\frac{\partial\dot{\omega}}{\partial V_r}\Big|op \cdot \Delta V_r + \frac{1}{J_T}\frac{\partial\dot{\omega}}{\partial \omega_r}\Big|op \cdot \Delta\omega_r + \frac{1}{J_T}\frac{\partial\dot{\omega}}{\partial \beta}\Big|op \cdot \Delta\beta \qquad \text{Eq. 3.31}$$

Reducing the equation can be written as:

$$\Delta\omega_r = \alpha\Delta V_r + \gamma\Delta\omega_r + \delta\Delta\beta \qquad \text{Eq. 3.32}$$

where, ΔV_r, $\Delta\omega_r$ & $\Delta\beta$ represent the deviations of the model from the operation points, V_{r0}, ω_{r0} & β_0 and the letters α,γ & δ represent the coefficients of the equation 3.31. The values of them are calculated from the following derivatives:

$$\alpha = \frac{\partial\dot{\omega}}{\partial V_r}\Big|op = \frac{1}{J_T}\left[\frac{\partial T_r}{\partial V_r} - N\frac{\partial T_g}{\partial V_r}\right] \qquad \text{Eq. 3.33}$$

$$\gamma = \frac{\partial\dot{\omega}}{\partial\omega_r}\Big|op = \frac{1}{J_T}\left[\frac{\partial T_r}{\partial\omega_r} - N\frac{\partial T_g}{\partial\omega_r}\right] \qquad \text{Eq. 3.34}$$

$$\delta = \frac{\partial\dot{\omega}}{\partial\beta}\Big|op = \frac{1}{J_T}\left[\frac{\partial T_r}{\partial\beta} - N\frac{\partial T_g}{\partial\beta}\right] \qquad \text{Eq. 3.35}$$

and describe the WT dynamics and their values rely on the wind speed and the partial derivatives of the power coefficient (C_p) with respect to λ & β at the operating points. The magnitude of α and δ are dependent on the wind speed (disturbance) and the pitch angle (input).

In the Laplace domain Eq. 3.32 becomes:

$$s\Delta\omega(s) = \alpha\Delta V(s) + \gamma\Delta\omega(s) + \delta\Delta\beta(s) \rightarrow \Delta\omega(s) = [\alpha\Delta V(s) + \delta\Delta\beta(s)]\frac{1}{s-\gamma}$$

Rewriting the previous equation, results to the following transfer functions which represent the reduced linear plant. The transfer function H1 models the dynamics that the wind speed (disturbance) introduce to the system and the transfer function H2 scales the behaviour of the pitch angle (input) to the plant states.

$$\boxed{H1 = \frac{\alpha}{s-\gamma} \qquad \& \qquad H2 = \frac{\delta}{s-\gamma}}$$

The Figure 3.15 below shows the block diagram representation of the model. Furthermore a comparison of the behaviour of this linear plant and the previous designed non-linear plant was conducted as well.

Worth to mention also that the defined system is stable, with poles of the transfer function lying on the left hand plane and values p1&p2=- -0.1068 (for H1&H2).

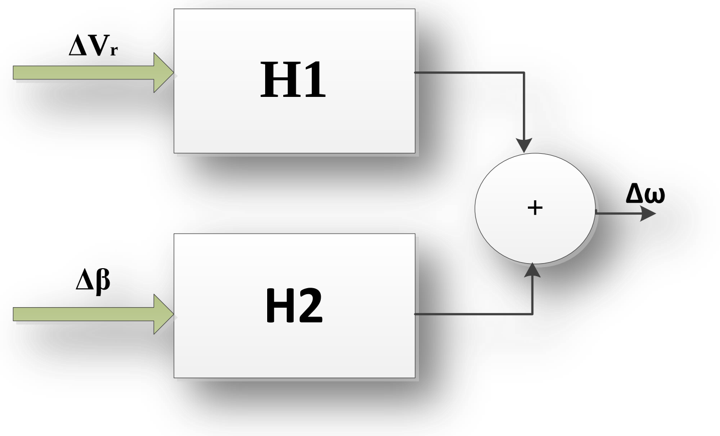

Figure 3.15 – Block diagram representation of the linear plant.

3.9.2. The linear model validation

Now that the linear plant is represented with a set of first order transfer functions it was tested around its operating points (V_{r0}=18m/s and β_0=14.89°) and expect for it to behave like the nonlinear one. The table below summarizes the conducted tests at the open loop system and comparisons that occurred to them with step as disturbance acting on the transfer function H1:

Table 3.1 – Test sequence (step as disturbance) between linear and nonlinear plant.

Number of test	V_r (disturbance)	β	ω_r linear maximum	ω_r nonlinear maximum	Results
Test 1	18→17	14.89	1.161	1.118	Figure 3.16
Test 2	18→19	14.89	1.445	1.447	Figure 3.17

Similar way like before, we test the linear open loop system with a pulse of amplitude higher and lower than the operational value. The system is expected to increase its speed and after the disturbance stop acting on it, the states should return back to its operational value. This will prove that the system behaves as it should base on its dynamics and that it is stable as system. The following table summarizes the tests that was conducted and shows the differences in the final values between linear and nonlinear system

Table 3.2 – Second test sequence (pulse as disturbance) between linear and nonlinear plant.

Number of test	V_r (disturbance)	β	ω_r linear maximum	ω_r nonlinear maximum	Results
Test 1	18→18.5→18	14.89	1.368	1.372	Figure 3.18
Test 2	18→17.5→18	14.89	1.217	1.228	Figure 3.19

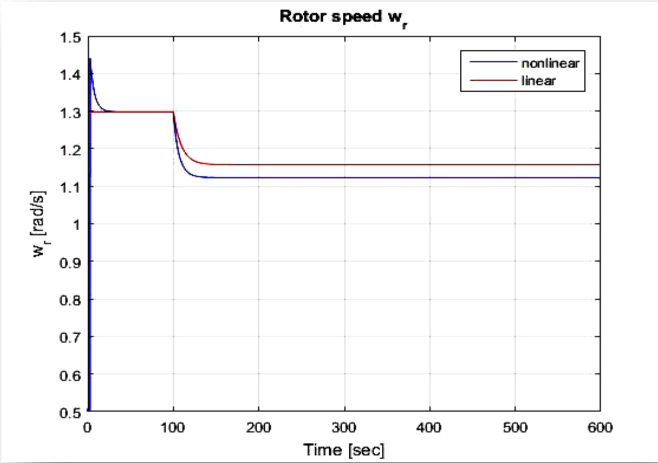

Figure 3.16 - Behavior of the linear (red) and nonlinear (blue) plant with disturbance from the operational point be Vr=17m/s at t=100s and for simulation time 600s.

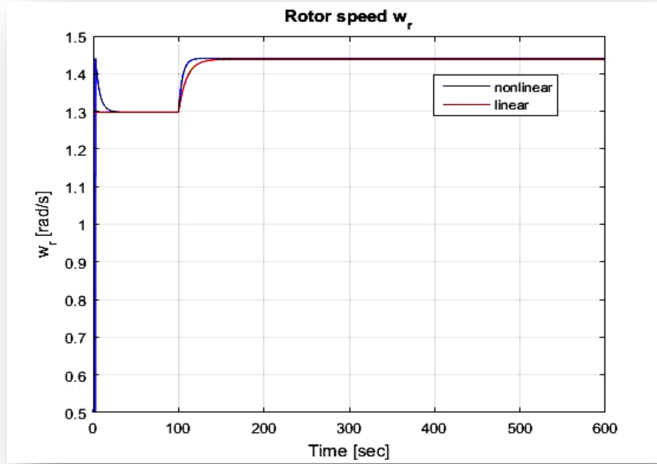

Figure 3.17 - Behavior of the linear (red) and nonlinear (blue) plant with disturbance from the operational point be Vr=19m/s at t=100s and for simulation time 600s.

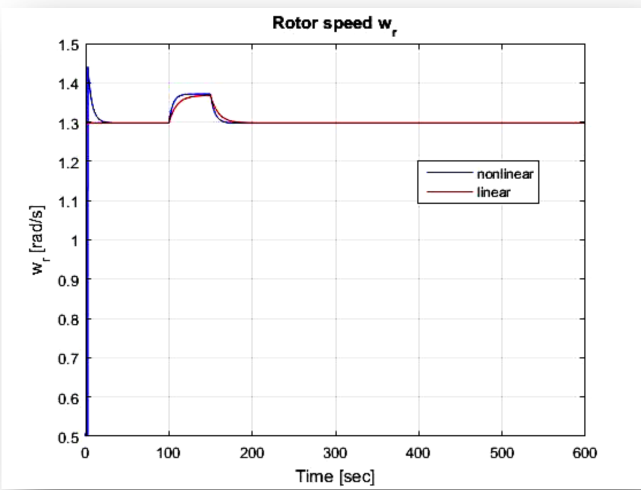

Figure 3.18 - Behavior of the linear (red) and nonlinear (blue) plant with pulse disturbance acting at t=100s until t=150s and with Vr=18.5 at this period.

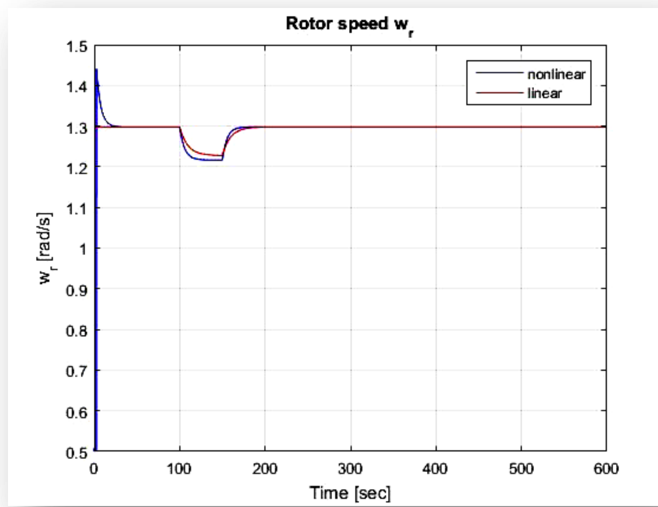

Figure 3.19 - Behavior of the linear (red) and nonlinear (blue) plant with pulse disturbance acting at t=100s until t=150s and with Vr=17.5 at this period.

As we can see from the validation tests, the linear model follows a logical behaviour and acts as the nonlinear plant when the two open loop models are compared under the same disturbance. Additionally, the system's stability is observable at Figure 3.18-3.19.

.

3.9.3. State space representation & validation

Now that the system is checked that behaves as it should, we will represent our transfer functions in the state space domain (continuous and discrete) and validate them as well. It was chosen for the system to work in the state space discrete domain because the controller works properly in this domain and also in discrete domain we can represent betters the small deviations from the operation point. Because the plant is a simple first order system the state space is simple as well and representing by scalar (or 1x1 matrices) with classic state space form:

$$\dot{x} = Ax + Bu$$

$$y = Cx$$

and with values:

SS1 (β - input system) - Eq.3.33

$$\dot{x} = [-0.1068]x + [1]u$$

$$y = [0.0089]x$$

SS2 (Vr – disturbance system) – Eq. 3.34

$$\dot{x} = [-0.1068]x + [1]u$$

$$y = [0.0155]x$$

For the controller design it is safe to transform our state space system from continuous to the discrete domain. This happens because the MPC controller works optimal in discrete domain. So the new state space in the discrete domain with sampling time Ts=0.1s and x_k stands for states deviations away from the linearization point and u_k for the pitch angle deviations and the incoming wind deviations from their operating points.

General discrete state space form:

$$x_{k+1} = A_d x_k + B_d u_k$$

$$y = C_d x_k$$

with values:

SS1 discrete 2 (β - input system) - Eq.3.34

$$x_{k+1} = [0.9894]x_k + [0.995]u_k$$

$$y_k = [0.0089]x_t$$

SS2 discrete 1 (Vr – disturbance system) - Eq.3.35

$$x_{k+1} = [0.9894]x_k + [0.995]u_k$$

$$y_k = [0.0156]x_k$$

The behavior of the two state space systems was validated against the linear and nonlinear systems with the results presented in the Figure 3.20 - 3.22 below. The disturbance that was implemented in the models had value of 18.5m/s. All the systems described above had the same reaction (rising) while the disturbance was affecting the systems and later were stabilized in the rated rotor's speed when the disturbance stops acting on them. Step input was implemented as well and the results were again satisfying.

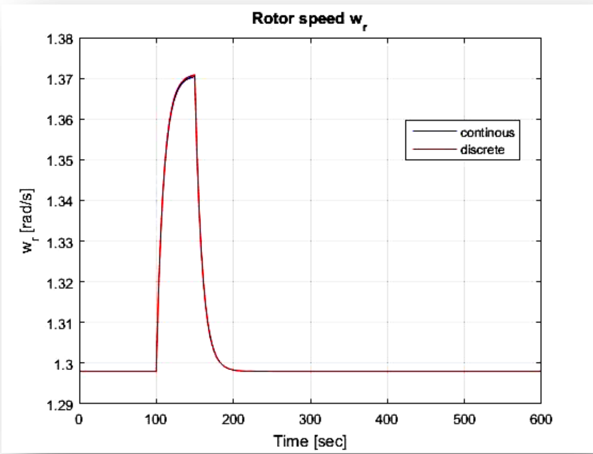

Figure 3.20 – Reaction of the continuous vs. discrete state space model under pulse disturbance of 18.5m/s for t=50s

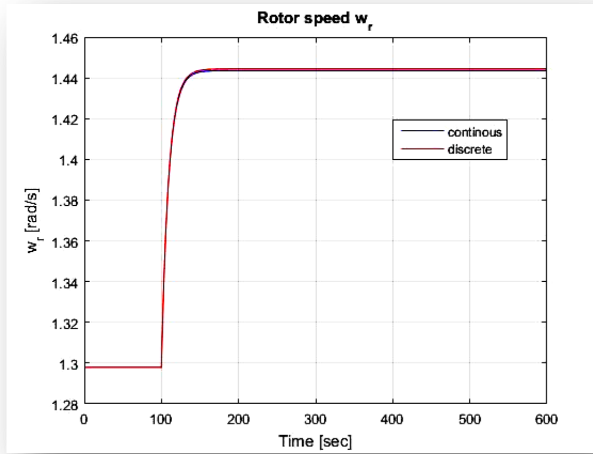

Figure 3.21 – Reaction of the continuous vs. discrete state space model under step disturbance of 19m/s from t=100s until the end of the simulation time

Figures 3.22-3.23 summarize the reaction of all the created models under the same disturbances to prove that they act in the same manner under the same disturbance (V_r=18.5m/s (pulse) and Vr=19m/s (step) simulation time 600s).

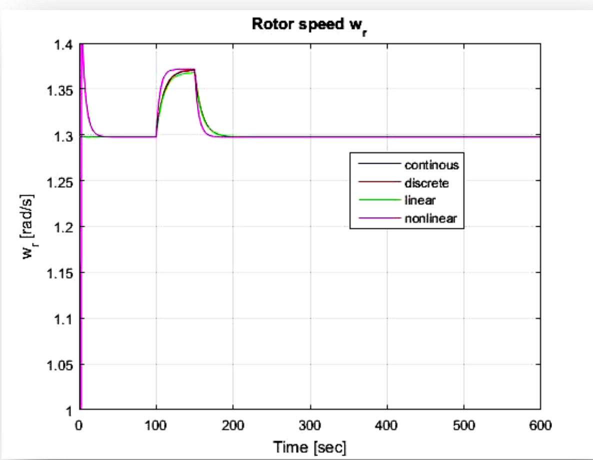

Figure 3.22 – Reaction of all the models under same pulse disturbance.

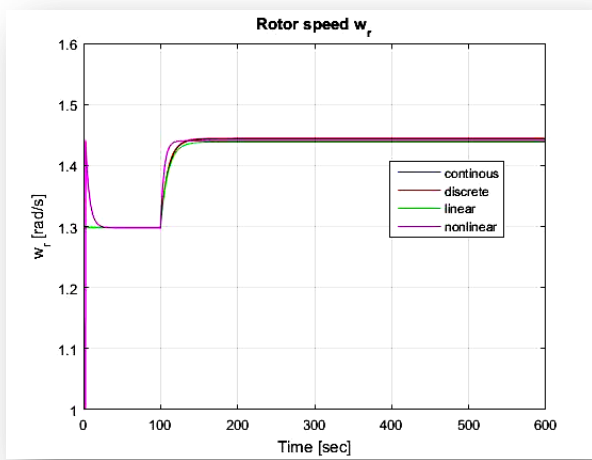

Figure 3.23 – Reaction of all the models under same step disturbance.

4. CONTROL PLAN & CONTROLLER DESIGN

In chapter 4, the design and the implementation of the controller occur. The receding horizon idea is explained. The parameters for the designed MPC controllers are explained, defined, tuned and then implemented. A comparison between the designed MPC and classic PI controller happens. Lastly we compare the results of implemented MPC in the nonlinear model with a baseline controller working in similar models. The control plan approach was designed based on [21, 27, and 29]

4.1. MPC - Receding horizon approach

The following figure sums up the whole concept of the receding horizon idea in model predictive control.

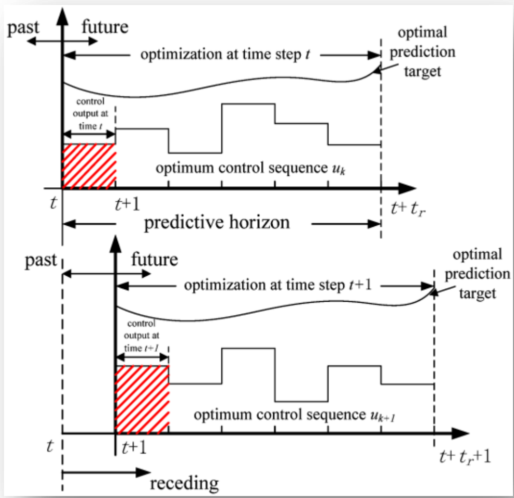

Figure 4.1 – Receding horizon operation concept. Top part shows the output at time t and the optimized outputs based on control output at time t. Bottom pictures illustrates the output at time t+1 and the optimized variables based o control output at time t+1 that they are different that the previous optimized ones [28].

The main concept of an MPC controller is that within a specified time horizon, so called prediction horizon the controller will predict the response of the system for a given value of input changes. At time [k] uses the system states and predicts the output. Additionally, at the same time, predicts the optimal control input that will respond to the optimal output of the system. It is possible to use a reference signal so the system tries to follow a specific, tracking output, but this is not used in this project.

The receding horizon theory refers to the changes that occur in the prediction (H_p) and control horizon (H_u) when these two are moving along with time. For instance, when from [k] the controller moves to [k+1] the prediction horizon is doing the same and moves to a new horizon noted as [k+1+H_p]. In this way it can always keep its length, H_p, for the whole simulation time. For the control horizon is the same, just the length of it is noted as H_u. The designed controller predicts (& optimizes) the changes in the input for the control horizon, but applies only the first optimal input to the system. At time [k] this is the control action, u_k. Then the controller is moving to time [k+1] and applies the u_{k+1} control move. This continues until the end.

In order to become more precise about the cost function, at the current time and state the controller solves an optimization problem with general form:

$$min\, J(k) = \sum_{k=0}^{Hp-1} Q(x_{k+1|k})^2 + \sum_{k=0}^{Hu-1} R\left(\Delta u_{k+1|k}\right)^2 \qquad \text{Eq. 4.1}$$

$$subjected\ to\quad x_{k+1} = Ax_k + Bu_k \qquad For\ k{=}0\ldots Hu \qquad \text{Eq. 4.2}$$

$$\Delta u_{k+1|k} \leq S \qquad For\ k{=}0\ldots Hu \qquad \text{Eq. 4.3}$$

$$x_{k+1|k} \leq x_{max} \qquad For\ k{=}0\ldots Hp \qquad \text{Eq. 4.4}$$

where, $x_{k+1|k}$ is the predicted by our controller future state, based on calculation at current state. $\Delta u_{k+1|k}$ is the predicted control input u_{k+1} based on calculations of the u_t. The Q, R $\epsilon\ \mathbb{R}^{n,\ m}$ are weight parameters and define how much the controller will penalize the minimization of the state or the control input respectively. Equation 4.2 – 4.4 are the constraints and they have to be followed by the controller during the optimization procedure or penalization will occur. The weight parameters (Q, R) and the horizons (H_p, H_u) as well are the tuning parameters of the designed controller.

4.2. Control plan

The control plan is essential to create a good and robust controller. So the definition of the plan needs to be clear and right to the spot.

In the very beginning of the project the plan was to create an MPC controller, which together with LIDAR measurements, will be eligible to control the operation of the WT as well as keep the power production in maximum levels. In this aspect and based in limitations that occurred during the completion of the report, we create a reduced model as was presented and validated in Ch. 3.9. This model works at the rated region of the WT and identifies the deviations that our model's states have from its operational point (ω_{r0}=1.298 rads/s) when the system is disturbed from wind variations (Vr≠Vr0). Thus, the ultimate control object for this project is to control the deviations that occur to the rotor's speed of the designed system when disturbance (V_r) is applied to the system. Controlling these deviations it can be assumed that the ultimate goals of a WT control plan can be regulated as well.

The system is represented by two discrete state space models of the form:

$$x_{k+1} = A_d x_k + B_d u_k$$

$$y_k = C_d x_k$$

The systems SS1 and SS2 in discrete state space form:

SS1: $$\Delta\omega_{r_{k+1}} = A_{d1}\Delta\omega_{r_k} + B_{d1}\Delta\beta_k$$

$$\Delta\omega_{r_k} = C_{d1}\Delta\omega_{r_k} \quad \text{Eq. 4.5}$$

SS2: $$\Delta\omega_{r_{k+1}} = A_{d2}\Delta\omega_{r_k} + B_{d2}\Delta V_{r_k}$$

$$\Delta\omega_{r_k} = C_{d2}\Delta\omega_{r_k} \quad \text{Eq. 4.6}$$

In order to control the deviations that disturbance (SS2 system) creates to plant (SS1 system) when it deviates away from its operational point (V_{r0}=18m/s.) a controller that will derive and solve the following optimization problem for a prediction horizon needs to be created:

$$min_{J(k)} \sum_{k=0}^{Hp-1} Qx_k{}^2 + \sum_{k=0}^{Hu-1} R\Delta v_k{}^2 + \sum_{k=0}^{Hp-1} Pz_k{}^2 + Q_F x_{Hp} + R_F \Delta u_{Hu-1} + P_F z_{Hp} \quad \text{Eq. 4.7}$$

Subjected to

$$x_{k+1} = A_{d1}x_k + B_{d1}u_k, \quad k = 0 \ldots H_p - 1 \quad \text{Eq. 4.8}$$

$$z_{k+1} = z_k + x_k T_s, \quad k = 0 \ldots H_p - 1 \quad \text{Eq. 4.9}$$

$$u_{min} \le u_k \le u_{max,} \quad k = 0 \ldots H_u - 1 \quad \text{Eq. 4.10}$$

$$u_k - u_{k-1} \le ST_{s\,,} \quad k = 0 \ldots H_u - 1 \quad \text{Eq. 4.11}$$

In the Eq. 4.7 it is observable that the defined cost function is divided in three different parts. The first part minimizes the future states of the plant (SS1 – $\Delta\omega_r$). The second part minimizes the deviations between the control actions, as $\Delta u_k = u_k - u_{k-1}$. The last part minimizes the integral error that is created from the disturbance to the system. This part needs to be added in order the controller being able to handle the error that is created from the unknown for it disturbance. Additionally to the regular cost, the terminal state costs that penalizing the last actions of the controller. While the controller minimizes the cost function (Eq. 4.7) at every step, it has to follow the constraints (Eq. 4.8-4.11) of the problem. The first two are the dynamic constraints (regarding the output of the system) and the rest are inequality constraints (regarding the control action).

In the previous equations Hp, Hu and Ts represent the prediction and control horizon and the sampling time of the controller respectively. Also it worth to say that for Eq. 4.7 - 4.11 the control and the prediction horizon they have equal size.

The tuning parameters Q, R, P and Q_f, R_f, P_f are the weights of the cost function and based on their values the controller choose which action will be penalized more and which less during the whole optimization procedure. These are the tuning parameters of the controller that together with the value of the prediction horizon define how the controller will act.

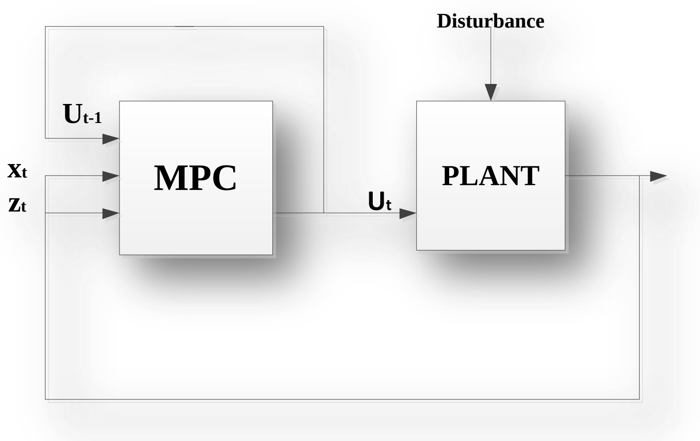

Figure 4.2 – The designed MPC controller's input and outputs based on the control plan. Inputs for the controller is the previous control action, u_{k-1}, the state xt and the integral state error of the plant, z_k

4.3.Implementation

For investigating different scenarios about the MPC approach in controlling the defined linear model, three different MPC controllers have been created and examined in this section. The controllers were created through CVXGEN (Ch. 2.4). The external program generated a custom convex optimization solver (the core part of the MPC controller) based in the system's states and the optimization problem (Eq. 4.7 - 4.11). This solver was implemented in Simulink and the needed parameters were tuned. The tuning procedure for the weight parameters is done with the trial and error method.

The three different cases were analyzed to understand the role of the prediction horizon in the controller design. Every designed controller has different defined prediction (and control) horizon. The three prediction horizons have length [20, 10 and 2 seconds] for the three designed controllers respectively.

4.3.1. MPCs and simulations

The figures below summarize the reactions of the three close loop systems, with the designed controllers acting on the linear system. The disturbance is a step signal with amplitude of 19m/s (while V_{r0}=18m/s) and was acting in the system at 100 seconds while the simulation time is 600seconds.

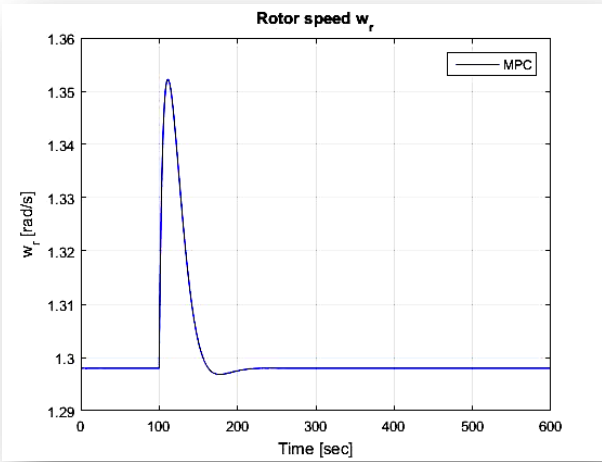

Figure 4.3 – Reaction of the system under the influence of the first designed MPC with prediction horizon of 20 seconds, with step disturbance of 19m/s.

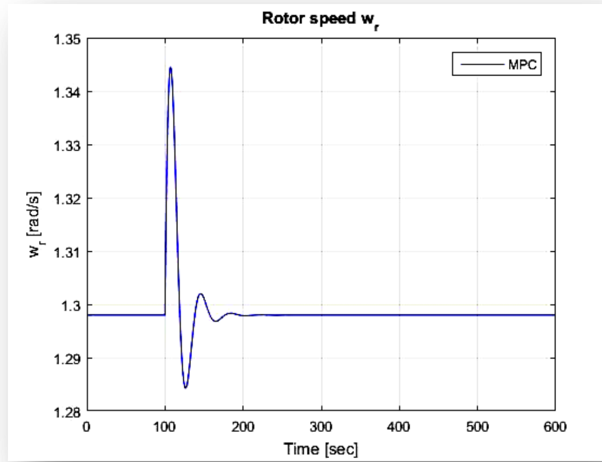

Figure 4.4 – Reaction of the system under the influence of the second designed MPC with prediction horizon of 10 seconds, with step disturbance of 19m/s.

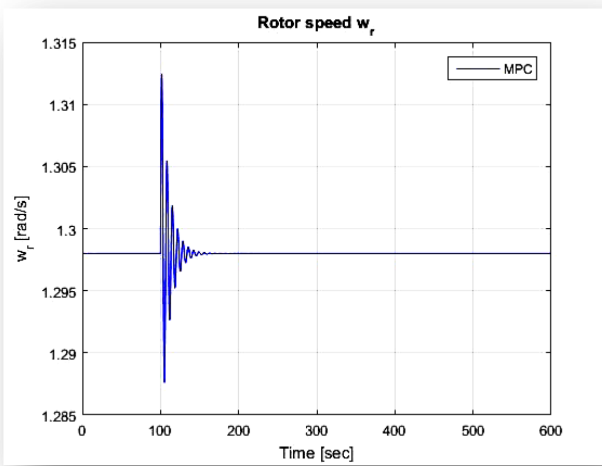

Figure 4.5 – Reaction of system under the influence of the third designed MPC with prediction horizon of 2 seconds, with step disturbance of 19m/s.

The Figure 4.3 shows the output of the close loop system (ω_r) for the designed MPC with prediction horizon (and control as well) of 20 seconds. As it is observed, the controller brings the system back to its steady state and limits the overshoot to less than 4% as well (see Figure 3.17 for same disturbance without controller). A thing to mention here is that the controller seems dull. This can be explained as the prediction horizon is long, the controller acts “lazily” as it understands that it has enough time to optimize and is not in rush.

In contrast with the previous MPC, the second designed MPC (with prediction horizon of 10 seconds) seems to act faster as it brings the system’s output to its operational point faster. This fast reaction of the controller tends to create a small undershoot. Additionally, it limits even more the overshoot to less than 3.5% of the steady state value.

Lastly, the third designed MPC with prediction and control horizon of 2 seconds seems to be the more appropriate one. The output of the system has the least overshoot (less than 2%) and despite the small oscillations (are really small that can be considered neglectable) it brings the system’s state at the operational point in less than 10 seconds. A thing to mention here is that the controller acts so fast that controls aggressively the system (as result it has the oscillations).

The tuning procedure (trial and error method was used) of the three designed controller addressed some interesting results. Big values in the weights of the system’s state (Q and Q_f) was driving the system to have bigger overshoot. Especially, when the final state cost (Q_f) had values over 100 it was creating a constant error to the systems output. Oppositely, small values were minimizing this error. The control action (R & R_f) weights affect the system as it follows. Small values for them was reducing the settling time while higher values was increasing it and was also creating fluctuations in the begging of the simulation without even the disturbance occurring. Both values need to be between 0 and 1.

Lastly the integral error weights (P and P_f) was probably the values that affecting more the system. Starting with the final integral error cost that for small values was creating a permanent bias to the system but high values was making the system slower. The integral error weight (P) with high value was reducing the system’s error but at the same time was making the controller more aggressive.

The following table summarizes the values for the weights parameters that were used to tune the MPC controllers:

Table 4.1 – Tuned parameters for the designed MPC controllers with different prediction horizons.

Parameters	MPC 1 (pred. hor. 20)	MPC 2 (pred. hor. 10)	MPC 3 (pred. hor. 2)
Q (state cost)	0.1	0.01	0.001
Q_f (final state cost)	10	1	0.1
R (control cost)	0.9e-3	0.9e-5	0.9e-6
R_f (final control cost)	0.9	0.09	0.09
P (integral cost)	10	100	500
P_f (final integral cost)	100	1000	5000

The tuned controllers were also checked under stochastic wind in order to check the ability of the designed MPCs in continuously changes of the disturbance. The range of the values for the wind distribution varies from 14 – 21m/s (based on wind values applied in [16]). As was expected the all three designed MPCs were able to control the system despite the wind variations and keep the close loop system's output close to the operational point (1.298 rads/s).

A thing to mention from these tests is the intensity of the controlled outputs. As it is observed in Figure 4.6 the output has less intensity compare to the other ones. Therefore, as the prediction horizon is reducing, the intensity of the system's output is getting bigger. As the Figure 4.8 shows, the faster controller has much bigger intensity. As it was mentioned before and validated here as well, the last designed controller seems to control the system in a more aggressive way compare to the other designed controllers, yet is the more robust one.

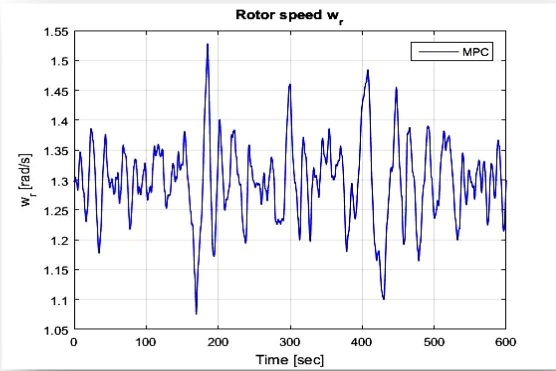

Figure 4.6 – Reaction of the system under the influence of the first designed MPC with prediction horizon of 20 seconds, with stochastic wind as disturbance.

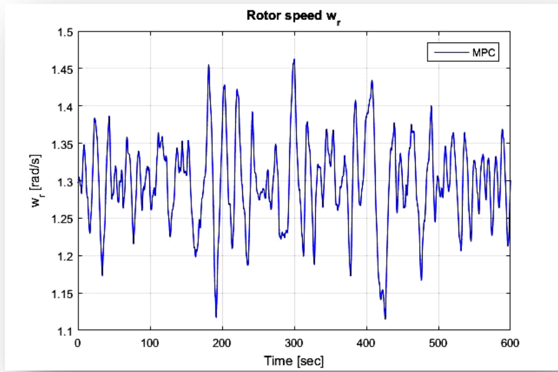

Figure 4.7 – Reaction of the system under the influence of the second designed MPC with prediction horizon of 10 seconds, with stochastic wind as disturbance.

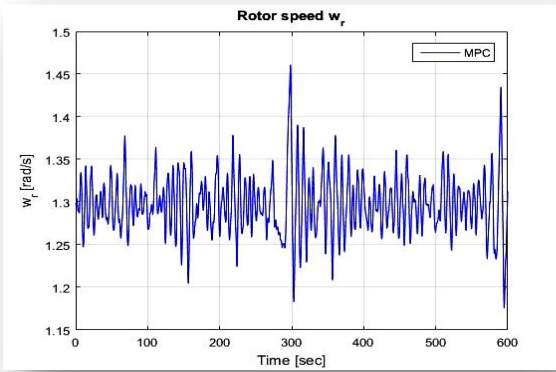

Figure 4.8 – Reaction of the system under the influence of the third designed MPC with prediction horizon of 2 seconds, with stochastic wind as

4.3.2. MPC vs. PI

A comparison between simple PI controller and the designed MPCs occurred. The PI controller was tuned under the optimal values for less possible overshoot and settling time. This comparison's goal is to show if advance control approach (MPC) is reliable enough as the classical control approaches and highlight their differences.

The figures below illustrate the first stage of the comparison, under step signal of 19m/s. disturbing the system's states.

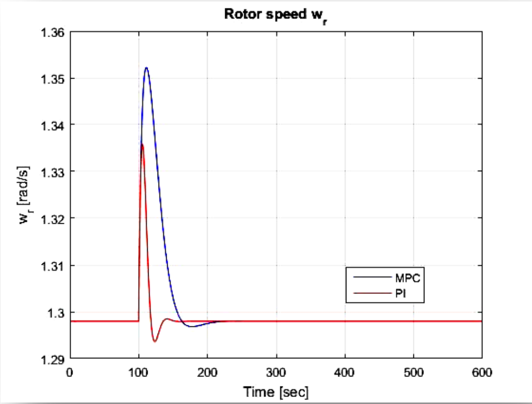

Figure 4.9 – Comparison between first designed MPC and PI controller, with step as disturbance acting on the system.

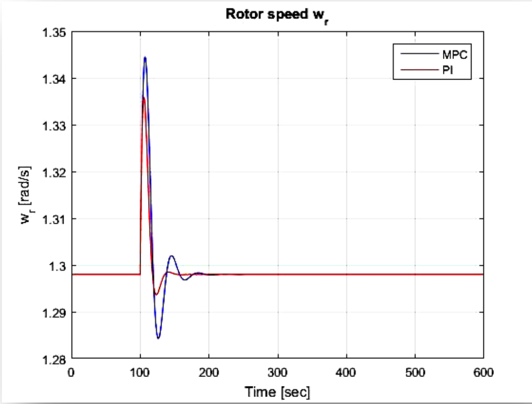

Figure 4.10 – Comparison between second designed MPC and PI controller, with step as disturbance acting on the system.

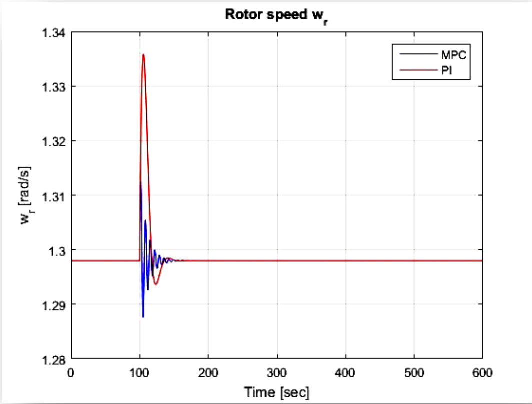

Figure 4.11– Comparison between third designed MPC and PI controller, with step as disturbance acting on the system.

In the first figure we can see that the PI is more robust and faster as well compared to the first designed MPC. As it was mentioned before this MPC considered being a slow controller because of its large horizon. Figure 4.10 shows the PI and the second designed controller comparison where the reaction of the system's output is almost the same. The controllers are equally robust with only difference; the overshoot of the MPC is slightly bigger. This means that the reduction of the horizon made the designed controller work as robust as the PI, despite as small sensitivity that created to it (undershoot) due to its faster reaction. In the last figure (Figure 4.10) it is observable that the MPC with the smaller horizon (2 seconds) is becoming more robust than the PI. But the aggression of the controller is observable again (small fluctuation).

A sum up shows that both controllers have the almost the same result to the system's output. Both control approaches have the same reaction in the disturbance compensation with main characteristic that the control of the MPC seems to becoming more aggressive as the horizon getting smaller.

The second stage of this comparison occurred under stochastic wind as disturbance. The results are illustrating in the figures below.

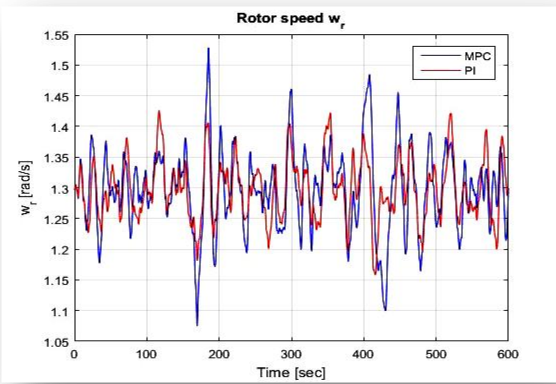

Figure 4.12 – MPC (20 seconds prediction horizon) vs. PI controller and system's reaction under stochastic wind disturbance.

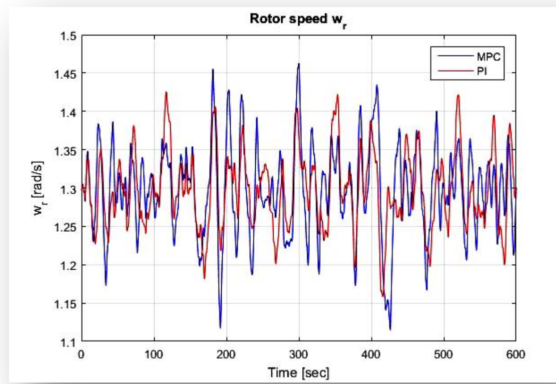

Figure 4.13 – MPC (10 seconds prediction horizon) vs. PI controller and system's reaction under stochastic wind disturbance.

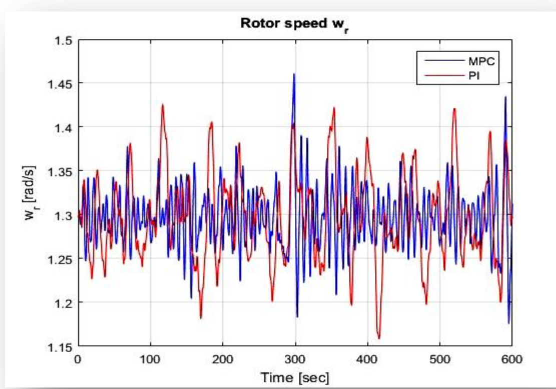

Figure 4.14 – Last designed MPC vs. PI controller and system's reaction under stochastic wind disturbance.

From the figures below it is easier understandable the main result of this comparison. The designed MPCs' (and especially the last, Figure 4.14) intensity in the system's output. This intensity is explained as the designed controllers tend to be more aggressive compare to the PI controller that controls in a smoother manner the disturbances that occur to the system.

4.3.3. PSD analysis for MPC & PI

Power spectrum density or PSD is a mean for signal analysis. A PSD can provide useful information for a characterized random signal (such as the stochastic wind) and its amplitude in the frequency domain. This type of analysis can help in the comparison between PI and MPC. Through this analysis it is observable which of the two signals contains, more harmful for the system, energy.

PSD analysis is achieved directly through Fast Fourier Transformation (FFT) and the results are presented below.

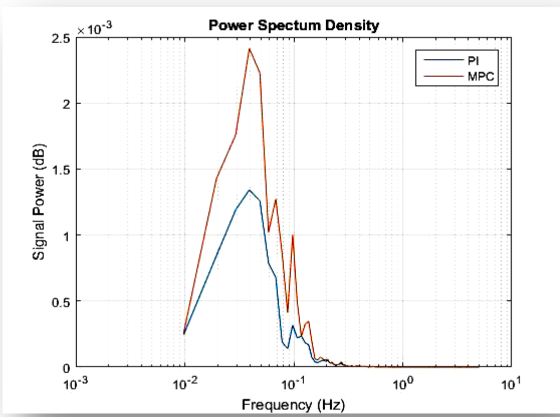

Figure 4.15 – Controlled signal's power expressed in the frequency domain for PI and MPC with horizon of 20seconds.

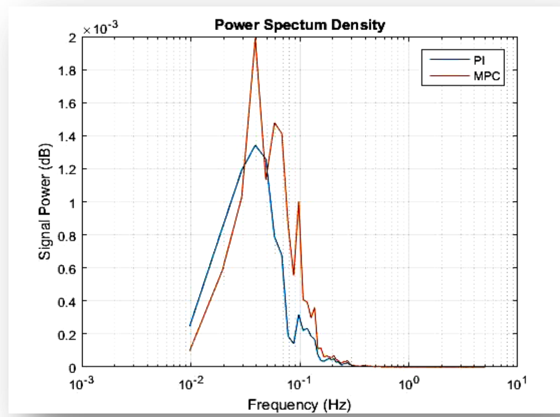

Figure 4.16 - Controlled signal's power expressed in the frequency domain for PI and MPC with horizon of 10seconds.

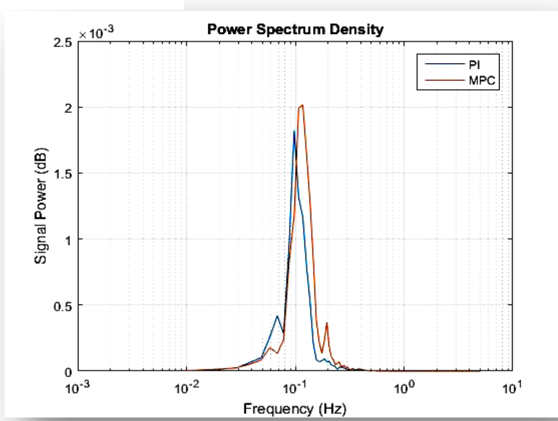

Figure 4.17 – Comparison of the controlled signal's power of the PI and the last designed MPC in the frequency domain

The Figure 4.15 shows that the amplitude of the signal produced by the designed MPC (20 seconds horizons) is higher compared to the one from the PI. This means that for the region 0.01 to 0.1Hz the controlled signal from the MPC contains more power. This higher amplitude can be harmful for the system as the additional power can be translated as additional noise. Additional noise can produce extra, unwanted vibrations which are something to avoid. The same in Figure 4.16 where the second designed MPC, despite the reduction of the horizons, still introduces higher amplitude signal to the designed system

In the last figure (figure 4.17) on the other hand the results differ. The further reduction of the horizon, despite that increase the intensity, decreases the range and the amplitude of the controlled signal. From the figure it is observed that both controllers have almost the same power in their signals.

To summarize the results of the PSD comparison, it can be said that the large horizons in the MPC design introduces signal with higher power amplitude. This kind of signals should be avoided as they can harm the system with vibrations. The last designed MPC despite that being more aggressive than the PI, contains the same power in its control signal like the PI.

4.3.4. MPC and nonlinear model

As the goal of the project was to apply an advance control method in the created nonlinear model, after the comparison with simple PI controller, was decided that the MPC controller with prediction horizon of two seconds was the more suitable for the nonlinear system.

The figure below shows the reaction of the designed nonlinear model under the MPC control and stochastic wind as disturbance.

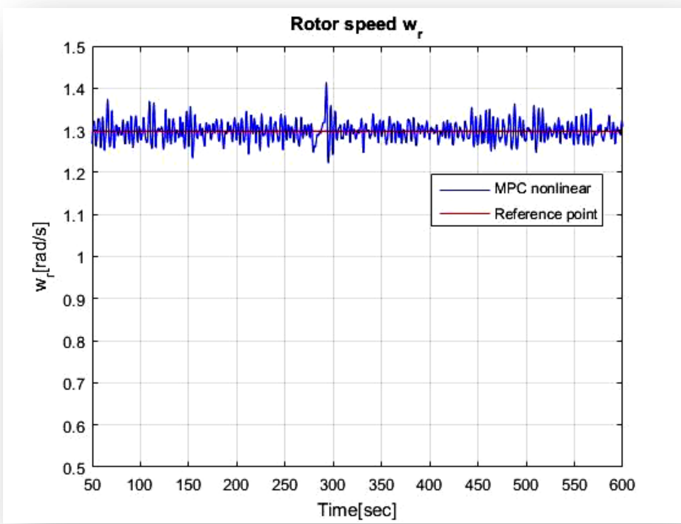

Figure 4.18 – Reaction of the nonlinear system in stochastic wind disturbance, under the influence of the MPC controller with prediction horizon of 2 seconds.

As the figure shows, the MPC handles the fast and large wind variations that try move the system away from its operational point. Again, the designed controller's intensity in compensating the disturbance is intense, yet efficient.

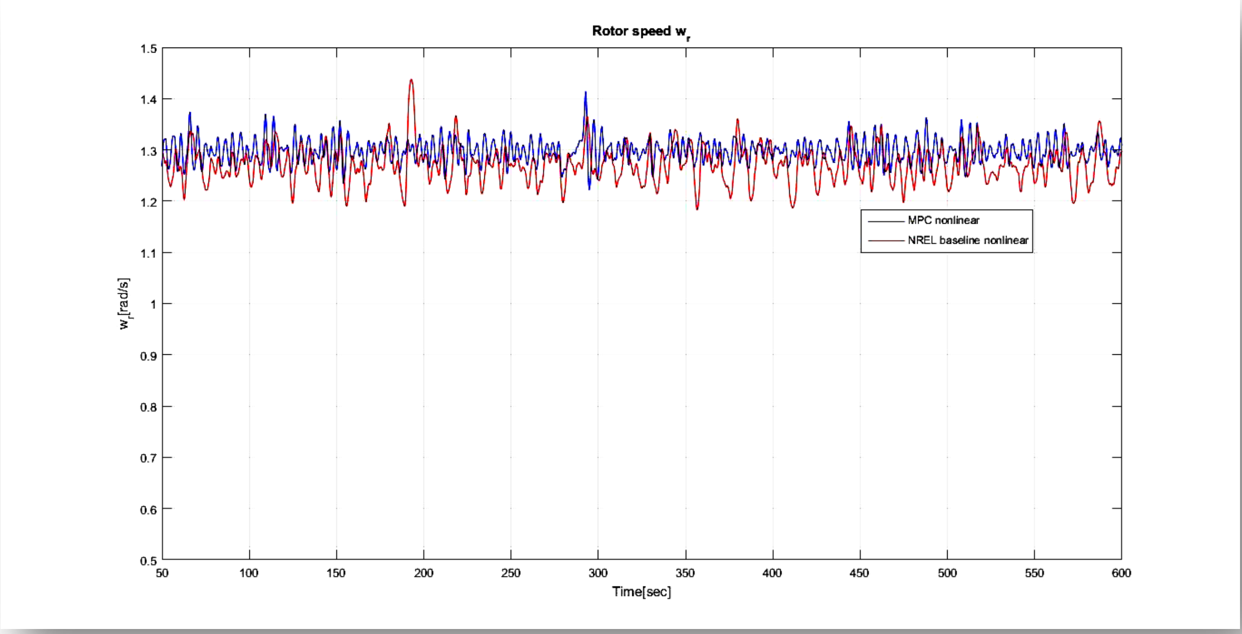

Figure 4.19 – Designed MPC acting on the reduced model vs. baseline controller acting on the proposed in [16] full scale model.

Last part of this project is the comparison between the designed MPC and a baseline controller [16]. The Figure 4.19 summarizes the reaction of the systems' output under the influence of both controllers. For one more time, the designed MPC (with prediction horizon of two seconds) is robust but in order to be so it seems to control the deviations with higher intensity in its signal. Oppositely, the baseline controller results are less robust (higher peaks), but the controlling procedure looks smoother than the designed MPC's.

5. CONCLUSION & FUTURE WORK

The following, last, chapter summarizes the results of the simulations that we conduct for the completion of this thesis. Additionally further improvements are addressed as well.

5.1.Discussion of the results

An interpreted version of the model proposed in [16] was defined and validated with respect to its output. The model was derived under specific conditions and around its rated values (V_r=18, β=14,89 & ω_r=1.298) for the disturbance, the input and its state respectively as it is shown in chapter 3.9. A linear model was derived and validated as well through different type of disturbances and with respect to the designed nonlinear model and its dynamics.

Continuously, a control plan and an optimization problem were defined (Eq. 4.7-4.11). With the contribution of external program (CVXGEN) three different MPC controllers able to minimize the cost function was created and its optimized control actions were used as control input for our system. The controller was tuned under different type of disturbances (step & stochastic wind) to investigate if it can operate and control the linear and the nonlinear models that have been created before.

Additionally, comparison between the designed MPC and simple PI controller acting to the linear model occurred. Also, a PSD analysis to the output signal of the MPC and the PI controllers was occurred and show that the MPCs' signal has higher power amplitude than the regular PI, for large prediction horizon length. In the end, a comparison between the designed MPC acting on the nonlinear s plant and the baseline controller acting on the proposed model happened to show that the MPC can control the nonlinear system in the same manner.

The followed statement summarizes the conclusion of this project:

A model predictive controller can be a robust controller for a WT system, without having the knowledge of future disturbances. It can handle and reduce the system's deviation from the operational point. As advanced control approach, model predictive controller is built based on the model of the system that is used for. Therefore, the simpler the model, the less exploitation of the designed controller abilities. Additionally, an advance control approach, such as MPC, despite that the model is reduced; it will try to predict and optimize the output of the system. This was observable in Figures 4.14 & 4.19 where the deviations in the system that is controlled by the MPC are smaller, compare to the other controller (PI &baseline). But in simple systems this extra action can make the controller aggressive with more intensity and harder to tune.

This statement can be separated in two parts, regarding the modelling procedure and the control designing. From the modelling point of view, it is understandable that the defined model, despite that represent the WT dynamics really well, it lacks of complexity. Based on this, its control approach doesn't need to be complex in order to be efficient. The deviations that occur to the created system's states can be smoothly handled by a simple control method (i.e. PI). Also, as long as the expectations of the model are not overestimated classic control methods can be reliable and easy to achieve.

For the control approach, advance control methods, such as MPC, can be implemented in a simple system. The implementation part (Ch.4.3) showed that model predictive controllers with fine tuning can be robust. The PSD analysis shows interesting results as well. Meaning, the faster and more robust the controller the less unwanted noise is introduced to the system's input signal as well. This can be an asset for the designed MPC, because an optimal tuning can lead to optimal results.

The tuning procedure although is a harder (time and computation) compare to the classic control approach. Additionally the MPC calculations cost can be high as well (when the controller solves the optimization problem online). These two factors need to be considered because the simplicity of the easy tuned PI controller seems to be an easier and more logical approach for the reduced system.

A thing to mention is that the best fitted controller (MPC with horizons of 2 seconds) controls the system with more intensity. This lies to the fact that an advance control method tries to continuously optimize the output without considering the system's simplicity. This drives the controller to operate harder for no realistic reason.

5.2.Discussion of future improvements

Future improvements in this project can also be categorized in two different sections. Improvements in the model approach and improvements in the advance control method approach.

For the model approach, as it was stated before, the simplicity of the model doesn't help in the advance control approach. A more detailed model approach based on the modelling explained in the Chapter 3 can be considered as advantage. More inputs and states can make a more detail and precise model. Additionally to this model, measurements of the incoming wind (such as LIDAR measurements) can make the model even more advanced and the control object more complex but at the same time more precise.

Also, the linearization of the model can change as well. For the case that was analysed in this project, the linearization occurred around one point. This can be change and a more complex approach can be linearized around different operating points, in the different control regions of the WT.

For the control approach, MPC seems to be a good approach. This control method, as the name states, is a model based approach. If the model is more advance then the controller is becoming more advance as well. Additionally, when the model can include knowledge of the upcoming future, this can exploit the controller's full potential as it was stated in similar work section. The MPC can introduce optimal control in complex systems and lead to reduction of mechanical loads and optimal energy production.

BIBLIOGRAPHY

Reports/Books/Chapters

[1] Energy Policies of IES Countries: Denmark Review, International Energy Agency, March 2011

[2] European Commission. Energy 2020 - a strategy for competitive, sustainable and secure Energy, European Union, March 2011

[4] The European Wind Energy Association, EU energy policy to 2050 - achieving 80-95% Emissions reductions, March 2011

[5] The European Wind Energy Association, Upwind - design limits and solutions for very large wind turbines, March 2011

[6] W. E. Leithead & B. Connor, Control of variable speed, Wind turbines: Design task, International Journal of Control, 73:13, 1189-1212, DOI: 10.1080/002071700417849, November 2010

[7] K. E. Johnson, L. Y. Pao, M. J. Balas, and L. J. Fingersh, Control of variable speed wind turbines, IEEE Control Systems magazine, June 2006

[8] M. Geyler, P. Caselitz, Robust multivariable pitch control design for load reduction on large WTs, European wind energy conference, May 2007

[9] Kathryn E. Johnson, Adaptive Torque Control of Variable Speed Wind Turbines, National Renewable Energy Laboratory (NREL), August 2004

[10] M. Mirzaei, H. H. Niemann, N. K. Poulsen, Robust model predictive control of a wind turbine, American Control Conference, June 2012

[11] E. A. Bossanyi. Individual blade pitch control for load reduction, Wind energy journal, April-June 2003

[12] D. Schlipf, J. Mann, A. Rettenmeier, P.W. Cheng, Model of the Correlation between LIDAR Systems and Wind Turbines for LIDAR Assisted Control, 16th International Symposium for the Advancement of Boundary-Layer Remote Sensing, 2012

[13] D. Schlipf, S. Schuler, P. Grau, F. Allgöver, and M. Kühn, Look-ahead cyclic pitch control using LIDAR, University of Stuttgart

[14] J. Laks, L. Y. Pao, E. Simley, A. Wright, N. Kelley, and B. Jonkman, Model predictive control using preview measurements from LIDAR, 49th AIAA Aerospace Sciences meeting including the New Horizons Forum and Aerospace Exposition, 2011.

[15] F. Dunne, L. Y. Pao, E. Simley, A. Wright, N. Kelley, and B. Jonkman, Adding feedforward blade pitch control for load mitigation in wind turbines: Non-causal series expansion, preview control, and optimized fir filter methods, American Institute of Aeronautics and Astronautics & NREL

[16] J. Jonkman, S. Butterfield, W. Musial, and G. Scott, Definition of a 5-MW Reference Wind Turbine for Offshore System Development, Technical Report, National Renewable Energy Laboratory, February 2009

[21] E. A. Bossanyi, The design of closed loop controllers for wind turbines. Wind Energy Journal, Volume 3 Issue 3, July/September 2000

[23] A. K. Scholbrock, P. A. Fleming, L. J. Fingersh, A. D. Wright, D. Schlipf F. Haizman and F. Belen, Field Testing LIDAR Based Feed-Forward Controls on the NREL Controls Advanced Research Turbine, NREL, New Horizons Forum and Aerospace Exposition Grapevine, Texas January 2013

[25] N. Jenkins T. Burton, D. Sharpe and E. Bossanyi, Wind Energy Handbook, J.Wiley and Sons Ltd, 2001

[27] M. Soltani, R. Wisniewski, P. Brath and S. Boyd, Load Reduction of Wind Turbines Using Receding Horizon Control, September 2011

[28] C. Hu, S. Luo, Z. Li, X. Wang, L. Sun, Energy Coordinative Optimization of Wind-Storage-Load Micro grids Based on Short-Term Prediction, February 2015

[29] J.M. Maciejowski, Predictive Control with Constraints, 2002

Internet sources

[3] Annika Breidthardt, Reuters, "German government wants nuclear exit by 2022 at latest", 30 May 2011, Accessed: February 2016
http://uk.reuters.com/article/us-germany-nuclear-idUKTRE74Q2P120110530

[17] National renewable Energy Laboratory, Accessed: March 2016
http://www.nrel.gov/

[18] Science/Howstuffworks.com, Accessed: March 2016
http://science.howstuffworks.com/

[19] Electrical and Computer engineering (http://sustain.ece.ksu.edu/), Accessed: March 2016
http://sustain.ece.ksu.edu/pages/anemometer.php#

[20] Danish wind industry association, Accessed: March 2016
http://xn--drmstrre-64ad.dk/wp-content/wind/miller/windpower%20web/en/tour/wtrb/yaw.htm

[22] Naperville Central Science (https://thecentralscience.wikispaces.com/), Accessed: March 2016
https://thecentralscience.wikispaces.com/Wind+Turbines...Low-speed+shaft

APPENDIX

Part A: Simulink models

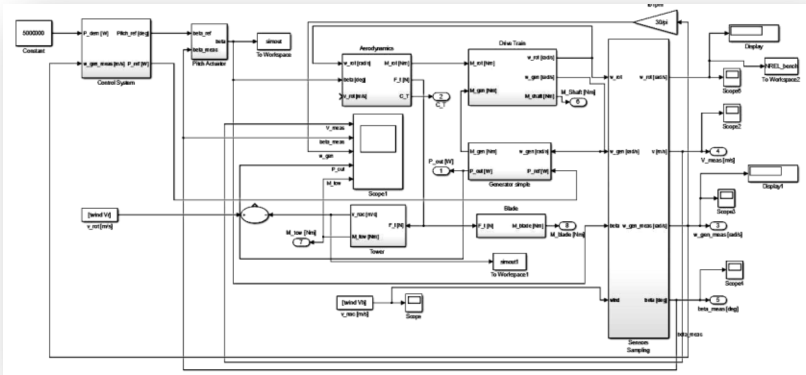

Figure – NREL 5MW nonlinear model Simulink model [16].

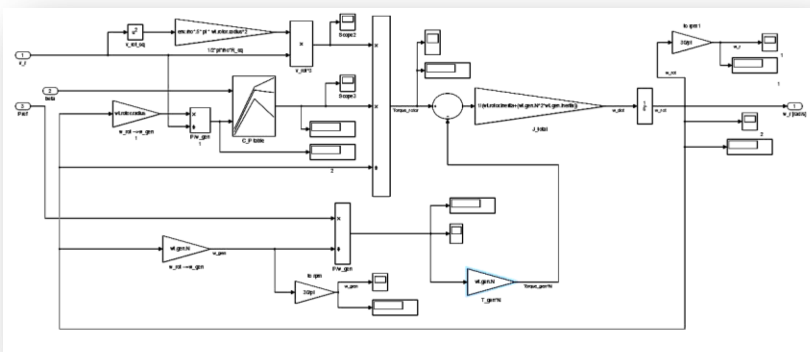

Figure - Designed nonlinear model, own figure & system.

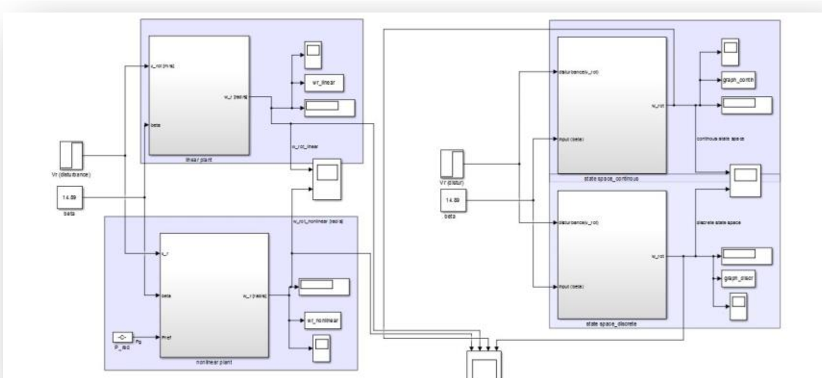

Figure – Validation of nonlinear, linear (left side), state space (continuous) and state space (discrete) system (right side).

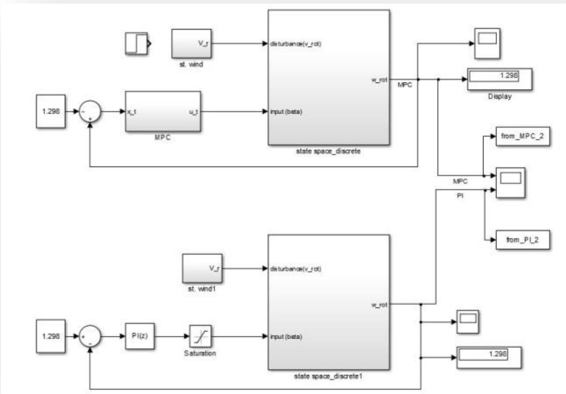

Figure – MPC vs. PI controlling the linear system with disturbance (stoch. wind and step).

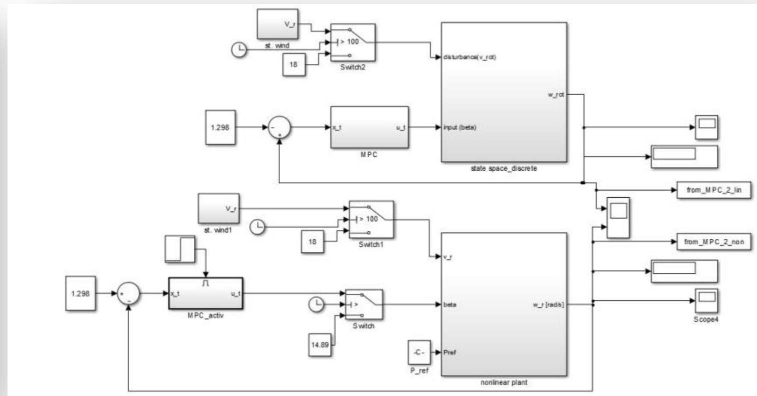

Figure – MPC acting on linear and nonlinear model.

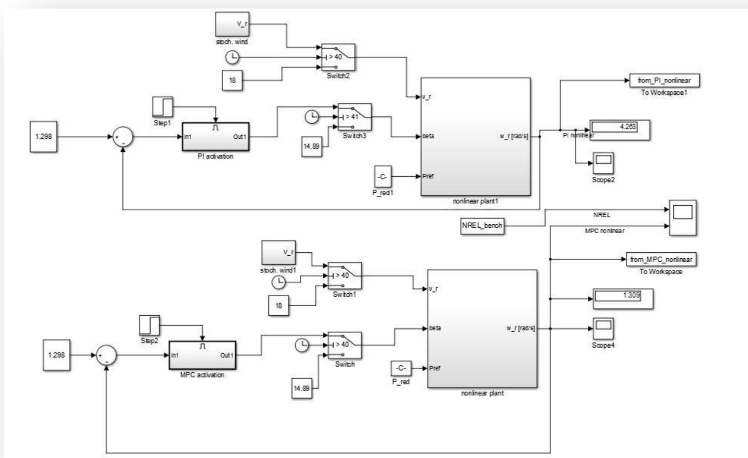

Figure – MPC nonlinear vs. PI benchmark nonlinear

Part B: CVXGEN code

```
dimensions
  T = 2     # horizon.
end

parameters
  A                 # dynamics matrix.
  B                 # transfer matrix.
  Q                 nonnegative  # state cost.
  R                 nonnegative  # input cost.
  P                 nonnegative  # input cost.
  Qf                nonnegative  # input cost.
  Rf                nonnegative  # input cost.
  Pf                nonnegative  # input cost.
  x[0]              # initial state.
  z[0]              # initial state.
  upr               # previous state trick.
  umin              # amplitude limit.
  umax              # amplitude limit.
  xmin              # amplitude limit.
  xmax              # amplitude limit.
  S                 # slew rate limit.
end

variables
  x[t] , t=1..T         # state.
  u[t] , t=0..T         # input.
  z[t] , t=1..T         # integral part
end

minimize
  sum[t=1..T-1](Q*square(x[t])) + Qf*square(x[T]) + ((R*square(u[0]-upr))+sum[t=1..T-1](R*(u[t]-u[t-1]))) + Rf*square(u[T-1]-u[T-2]) + sum[t=1..T-1](P*square(z[t])) + Pf*square(z[
subject to
  x[t+1] == A*x[t] + B*u[t],            t=0..T-1
  z[t+1] == z[t]+(0.1*x[t]),            t=0..T-1
  umin<=u[t]<=umax,                     t=0..T-1
  (u[t] - u[t-1])<= S*0.1,              t=1..T-1
end
```

Figure – Generated program for the MPC with prediction horizon of 2 seconds [24]

```
dimensions
  T = 10     # horizon.
end

parameters
  A                 # dynamics matrix.
  B                 # transfer matrix.
  Q                 nonnegative  # state cost.
  R                 nonnegative  # input cost.
  P                 nonnegative  # input cost.
  Qf                nonnegative  # input cost.
  Rf                nonnegative  # input cost.
  Pf                nonnegative  # input cost.
  x[0]              # initial state.
  z[0]              # initial state.
  upr               # previous state trick.
  umin              # amplitude limit.
  umax              # amplitude limit.
  xmin              # amplitude limit.
  xmax              # amplitude limit.
  S                 # slew rate limit.
end

variables
  x[t] , t=1..T         # state.
  u[t] , t=0..T         # input.
  z[t] , t=1..T         # integral part
end

minimize
  sum[t=1..T-1](Q*square(x[t])) + Qf*square(x[T]) + ((R*square(u[0]-upr))+sum[t=1..T-1](R*(u[t]-u[t-1]))) + Rf*square(u[T-1]-u[T-2]) + sum[t=1..T-1](P*square(z[t])) + Pf*square(z[
subject to
  x[t+1] == A*x[t] + B*u[t],            t=0..T-1
  z[t+1] == z[t]+(0.1*x[t]),            t=0..T-1
  umin<=u[t]<=umax,                     t=0..T-1
  (u[t] - u[t-1])<= S*0.1,              t=1..T-1
end
```

Figure – Generated program for the MPC with prediction horizon of 10 seconds [24]

```
dimensions
  T = 20     # horizon.
end

parameters
  A                 # dynamics matrix.
  B                 # transfer matrix.
  Q                 nonnegative  # state cost.
  R                 nonnegative  # input cost.
  P                 nonnegative  # input cost.
  Qf                nonnegative  # input cost.
  Rf                nonnegative  # input cost.
  Pf                nonnegative  # input cost.
  x[0]              # initial state.
  z[0]              # initial state.
  upr               # previous state trick.
  umin              # amplitude limit.
  umax              # amplitude limit.
  xmin              # amplitude limit.
  xmax              # amplitude limit.
  S                 # slew rate limit.
end

variables
  x[t] , t=1..T         # state.
  u[t] , t=0..T         # input.
  z[t] , t=1..T         # integral part
end

minimize
  sum[t=1..T-1](Q*square(x[t])) + Qf*square(x[T]) + ((R*square(u[0]-upr))+sum[t=1..T-1](R*(u[t]-u[t-1]))) + Rf*square(u[T-1]-u[T-2]) + sum[t=1..T-1](P*square(z[t])) + Pf*square(z[
subject to
  x[t+1] == A*x[t] + B*u[t],            t=0..T-1
  z[t+1] == z[t]+(0.1*x[t]),            t=0..T-1
  umin<=u[t]<=umax,                     t=0..T-1
  (u[t] - u[t-1])<= S*0.1,              t=1..T-1
end
```

Figure – Generated program for the MPC with prediction horizon of 20 seconds [24]